

UC Merced

UC Merced Electronic Theses and Dissertations

Title

Understanding regulation of immediate-early gene transcription in the brain.

Permalink

<https://escholarship.org/uc/item/0999h4rf>

Author

Dunn, Carissa Janette

Publication Date

2019

Copyright Information

This work is made available under the terms of a Creative Commons Attribution License, available at <https://creativecommons.org/licenses/by/4.0/>

Peer reviewed|Thesis/dissertation

UNIVERSITY OF CALIFORNIA, MERCED

Understanding regulation of immediate-early gene transcription in the brain.

A dissertation submitted in partial satisfaction of the requirements for the degree
Doctor of Philosophy

in

Quantitative and Systems Biology

by

Carissa J. Dunn

Committee in charge:

Professor Michael D. Cleary, Chair

Professor Chris Amemiya

Professor Masashi Kitazawa

Professor Stephen C. Noctor

2019

© Copyright
Carissa J. Dunn, 2019
All rights reserved.

The dissertation of Carissa J. Dunn is approved, and is acceptable in quality and form for publication on microfilm and electronically:

Dr. Chris Amemiya

Dr. Masashi Kitazawa

Dr. Stephen C. Noctor

Dr. Michael D. Cleary, Chair

University of California, Merced

2019

DEDICATION

This dissertation is dedicated to my ever-expanding network of support.

To my parents and siblings, you were my first team and you taught me about unconditional love. Despite my continuous efforts, I will never gain a more impactful piece of knowledge.

To my nieces and nephews, it is my sincerest hope that each of you approach the world with an open, curious mind. You all have something unique and beautiful to share, so make a purposeful effort to understand yourself at every stage of life.

To my extended family, closest friends, and loved ones, your continuous support enriches my life and I am eternally grateful for the ways in which you've helped me grow.

TABLE OF CONTENTS

Signature Page	iii
Curriculum Vitae	vi
List of Abbreviations	viii
List of Figures	x
List of Tables	xv
Acknowledgements	xvi
Abstract	xvii
Chapter 1: Introduction	
1.1 Motivation.....	1
1.2 Background.....	1
Chapter 2: Regulation of Neuronal Immediate-early Gene Transcription by H2A.Z Hypervariants	
2.1 Introduction.....	8
2.2 Results.....	9
2.3 Discussion.....	18
2.4 Future Directions.....	20
2.5 Materials and Methods.....	28
Chapter 3: Investigating How Activity-Induced Signaling Cascades Play Differential Roles in Regulating Neuronal Immediate-early Gene Transcription	
3.1 Introduction.....	33
3.2 Results.....	33
3.3 Discussion.....	41
3.4 Future Directions.....	42
3.5 Materials and Methods.....	45
Chapter 4: Conclusion	48
References	51

CURRICULUM VITAE

Carissa J Dunn

carissadunn92@gmail.com

Education

University of California, Merced **Merced, CA**
PhD, Quantitative and Systems Biology 2019

Davis and Elkins College **Elkins, WV**
B.S. Biology and Chemistry (double major) 2013

Publications

Dunn, C. J., Sarkar, P., Bailey, E. R., Farris, S., Zhao, M., Ward, J. M., ... Saha, R. N. (2017). Histone Hypervariants H2A.Z.1 and H2A.Z.2 Play Independent and Context-Specific Roles in Neuronal Activity-Induced Transcription of Arc/Arg3.1 and Other Immediate Early Genes. *eNeuro*, 4(4), ENEURO.0040-17.2017. doi:10.1523/ENEURO.0040-17.2017

Poston, R. G., **Dunn, C. J.**, Sarkar, P., & Saha, R. N. (2018). Persistent 6-OH-BDE-47 exposure impairs functional neuronal maturation and alters expression of neurodevelopmentally-relevant chromatin remodelers. *Environmental epigenetics*, 4(1), dvx020. doi:10.1093/eep/dvx020

Tyssowski, K. M., DeStefino, N. R., Cho, J. H., **Dunn, C. J.**, Poston, R. G., Carty, C. E., ... Gray, J. M. (2018). Different Neuronal Activity Patterns Induce Different Gene Expression Programs. *Neuron*, 98(3), 530–546.e11. doi:10.1016/j.neuron.2018.04.001

Scheidegger, A., **Dunn, C. J.**, Samarakkody, A., Koney, N. K., Perley, D., Saha, R. N., & Nechaev, S. (2019). Genome-wide RNA pol II initiation and pausing in neural progenitors of the rat. *BMC genomics*, 20(1), 477. doi:10.1186/s12864-019-5829-4

Research Experience

University of California, Merced **Merced, CA**
Graduate Student, Quantitative and Systems Biology 2014-2019
Regulation of immediate-early gene transcription in the brain.

Davis and Elkins College **Elkins, WV**
Undergraduate Research Assistant 2013
Glutathione levels in athletes with varying exercise regiments.

University of Utah **Salt Lake City, UT**
Summer Research Intern (SURP) 2012
Using a novel genomic pathway-based approach to discover a therapeutic against the Np63 oncogenic pathway.

West Virginia University*Summer Research Intern (INBRE)*

Determining the functional role of alternative splicing in cancer.

Morgantown, WV

2011

Teaching Experience**University of California, Merced***Teaching Assistant*

Undergraduate courses: Neurobiology, Genetics, Virology, Intro Biology

Merced, CA

2014-2019

Davis and Elkins College*Lead Tutor*

Subjects: Math (algebra-calculus), Biology, Chemistry, Physics, Environmental Science

Elkins, WV

2010-2013

Conferences and Presentations**UCM QSB Retreat 2018**Oral: H2A.Z.2 occupancy of promoter-proximal nucleosomes is required for Pol II pausing at *Arc/Arg3.1*.**Mariposa, CA****Society for Neuroscience 2016****San Diego, CA****Molecular and Cellular Cognition Society 2016**

Poster: Histone Hypervariants H2A.Z.1 and H2A.Z.2 Play Independent and Context-Specific Roles in Neuronal Activity-Induced Transcription of Immediate Early Genes.

San Diego, CA**SACNAS 2012**

Poster: Using a novel genomic pathway-based approach to discover a therapeutic against the Np63 oncogenic pathway.

Seattle, WA**Awards****UCM Grad Slam 2018**

Top 10 finalist

Merced, CA

LIST OF ABBREVIATIONS

IEG	Immediate early gene
Pol II	RNA Polymerase II
TSS	Transcription start site
MAPK	Ras/mitogen-activated protein kinase
CaN	Calcineurin
CamK	Calcium/calmodulin-dependent protein kinase
VSCC	Voltage-sensitive calcium channel
Bic	Bicuculline
4AP	4-aminopyridine
TTX	Tetrodotoxin
KD	Knockdown
pSer5	Phosphorylated Serine-5
Trip	Triptolide
DSIF	DRB sensitivity-inducing factor
NELF	Negative elongation factor
PMA	Phorbol myristate acetate
NPC	Neural progenitor cell
ICC	Immunocytochemistry
DCX	Doublecortin
MAP2	Microtubule-associated protein 2
BAF	Brg1/BRM associated factor
esBAF	Embryonic stem cell BAF
npBAF	Neural progenitor BAF
nBAF	Neuronal BAF
EdU	5-ethynyl-2'-deoxyuridine

DAPI	4', 6-diamidino-2-phenylindole
PI	Propidium iodide
UCM	University of California, Merced
NIEHS	National Institutes of Environmental Health Sciences
IACUC	Institutional Animal Care and Use Committee
DIV	Days <i>in vitro</i>
BSA	Bovine serum albumin
EGF	Embryonic growth factor
FGF	Fibroblast growth factor
PFA	Paraformaldehyde
CRTC1	CREB-regulating transcription coactivator 1
NFAT	Nuclear factor of activated T-cells
MEF	Myocyte enhancer factor
CHX	Cycloheximide
Aniso	Anisomycin
pERK	Phosphorylated ERK
PKC	Protein kinase C
PKA	Protein kinase A
eRNA	Enhancer RNA
CBP	CREB-binding protein
HAT	Histone acetyltransferase
SIK1	Salt-inducible kinase 1
SARE	Synaptic activity-responsive element
FSK	Forskolin
DRB	5,6-dichloro-1-beta-D-ribofuranosylbenzimidazole

LIST OF FIGURES

Figure 1-1. Illustration of calcium-dependent signaling pathways regulating activity-induced gene transcription in the brain.....	7
Figure 2-1. Amino acid differences between H2A.Z.1 and H2A.Z.2.....	9
Figure 2-2. H2A.Z.1 and H2A.Z.2 play context-dependent roles in activity-induced transcription of rapid IEGs. A. Representation of pre-mRNA levels for noted IEGs at different time points after two treatment regimens. Left, Bic+4AP treatment. Right, 48-h treatment with TTX followed by its washout for specified time periods in indicated groups of neurons as detected by qPCR and normalized to <i>Gapdh</i> . <i>N</i> = 4–7 for each time point. B. NanoString multiplexed gene expression data (heat maps) representing pre-mRNA levels in control and hypervariant-depleted neurons treated with Bic+4AP for indicated times. C. Heat maps representing pre-mRNA levels in control and hypervariant-depleted neurons treated TTX for 48 h followed by washout and collected at indicated times. D, E. Violin plots depicting pre-mRNA abundance of all rapid IEGs from hypervariant-depleted neurons compared to that of control neurons treated with Bic+4AP (D) or TTX for 48hr followed by washout (E) for indicated times. <i>N</i> = 3 for each treatment at all time-points. * <i>p</i> < 0.05 and ** <i>p</i> < 0.01 (Wilcoxon paired nonparametric test).....	10
Figure 2-3. H2A.Z hypervariant-specific RNAi has differential effects on activity-induced transcription of <i>Arc</i> . A. Representation of <i>Arc</i> mRNA level at 15 min after treatment with Bic+4AP in indicated neuronal groups as detected by qPCR and normalized to <i>Gapdh</i> . <i>N</i> = 3–4 for each group. B, C, Representation of <i>Arc</i> pre-mRNA level at different time points after treatment with Bic+4AP (B) or TTX+PMA (C) in indicated groups of neurons (5–6 d postinfection) as detected by qPCR and normalized to <i>Gapdh</i> . <i>N</i> = 3–4 for each time point. D. Representation of <i>Arc</i> pre-mRNA level at 15 min after treatment with Bic+4AP in indicated neuronal groups as detected by qPCR and normalized to <i>Gapdh</i> . <i>N</i> = 3. For all figures, * <i>p</i> < 0.05; ** <i>p</i> < 0.01; NS, not significant.....	11
Figure 2-4. H2A.Z.2 facilitates priming of the <i>Arc</i> promoter. A. Representative Western blotting of whole-cell lysate showing Ac-H2A.Z levels in neurons depleted of H2A.Z hypervariants as indicated. <i>N</i> = 3. B. Graphical map (not to scale) depicting relative position of ChIP primers near <i>Arc</i> TSS. C. Quantification of Ac-H2A.Z (normalized by total H2A.Z) binding to <i>Arc</i> TSS region in neurons treated as indicated, determined by ChIP. <i>N</i> = 4. Two sets of data in statistical comparison are represented by the position and the color of asterisk(s). D. ChIP data demonstrating binding of RPB1 to the <i>Arc</i> TSS region in control neurons or H2A.Z hypervariant-depleted neurons as indicated. <i>N</i> = 4. E. ChIP data	

demonstrating binding of pSer5-RPB1 to the Arc TSS in control and hypervariant-depleted neurons. $N = 3$. * $p < 0.05$ and ** $p < 0.01$13

Figure 2-5. H2A.Z.1 plays context-dependent roles in Arc transcription. A. Graphical representation of the level of Arc pre-mRNA at different time points after 1-h treatment with DRB (5,6-dichloro-1-beta-D-ribofuranosylbenzimidazole) followed by its washout for indicated time periods in the presence or absence of Trip in indicated groups of neurons (infected for 5–6 d) as detected by qPCR and normalized to Rn18s (18s rRNA; DRB inhibition-insensitive, Pol III-dependent transcription). Gray, green and red asterisk(s) or NS represent statistical comparison between control (Scrambled) responses and responses in Scrambled w/Trip, H2A.Z.1 KD w/Trip and H2A.Z.2 KD, respectively. Connecting brackets delineate other comparisons, shown in black asterisk(s) or NS. B. Similar dataset as in (A) except that control neurons or hypervariant-depleted neurons were treated with TTX for 48 h followed by its washout for indicated time periods. Two sets of data in statistical comparison are represented by the position and the color of asterisk(s) or NS. For both A, B. $N = 4–5$ for each time point; * $p < 0.05$ and ** $p < 0.01$. NS, not significant.....15

Figure 2-6. Effect of H2A.Z hypervariant depletion on transcription of delayed IEGs. A. Nanostring multiplexed gene expression data (heat maps) representing pre-mRNA levels in control and hypervariant-depleted neurons treated with Bic+4AP for indicated times. B. Heat map representing pre-mRNA levels in control and hypervariant-depleted neurons treated TTX for 48 h followed by washout and collected at indicated times. C, D. Violin plots depicting pre-mRNA abundance of all delayed IEGs from hypervariant-depleted neurons compared to that of control neurons treated with Bic+4AP (C) or TTX for 48 h followed by washout (D) for indicated times. $N = 3$ for each treatment at all time points. * $p < 0.05$ and ** $p < 0.01$ (Wilcoxon paired nonparametric test).....17

Figure 2-7. Preliminary investigation into amino acid differences between H2A.Z hypervariants. Representation of Arc pre-mRNA levels in neurons expressing exogenous constructs encoding normal H2A.Z.1, normal H2A.Z.2, three single point mutants, and three double mutants. Mature neurons were infected for 5 days and gene expression was induced by treating cells with Bic+4AP for 60 min; data expressed as fold change relative to *Gapdh* and compared to CD811A empty-vector control. $N = 3$20

Figure 2-8. Differential regulation of Arc expression in homeostatically challenged neurons after H2A.Z hypervariant depletion. Representation of Arc pre-mRNA expression in neurons treated with either TTX or Bic for 48hr followed by washout; samples collected 15 min after washout. Data represented as raw pre-mRNA values relative to *Gapdh*; $N = 3$; * represents $p < 0.05$21

Figure 2-9. Effect of H2A.Z depletion on neuronal development. A. shRNA-mediated knockdown of H2A.Z.1 (left) and H2A.Z.2 (right) in neuronal progenitor cells over the course of 4 passages; raw data represented relative to *Gapdh*; $N = 3$ for P1-P3 and $N = 1$ for P4; * represents $p < 0.05$, # represents $p = 0.064$ B. Representative ICC images showing expression of Nestin and DCX in NPCs (Day 0), and DCX and MAP2 in developing neurons (Day 9) depleted of either H2A.Z.1 or H2A.Z.2 before the onset of differentiation; notation at top represents time after the onset of differentiation.....**22**

Figure 2-10. Effects of H2A.Z hypervariant loss on expression of BAF complex subunits in neurons and NPCs. A. Representation of mRNA levels of neuron-specific BAF (nBAF) complex subunits in mature neurons depleted of either H2A.Z.1 or H2A.Z.2; data represented as raw mRNA values relative to *Gapdh*; $N = 3$; * represents $p < 0.05$. B. Representation of mRNA levels of NPC-specific BAF (npBAF) and nBAF complex subunits in NPCs depleted of either H2A.Z.1 or H2A.Z.2; data represented as raw mRNA values relative to *Gapdh*; $N = 4$**25**

Figure 2-11. Preliminary investigation into effects of hypervariant loss on neuronal differentiation. Quantification of fluorescent images taken of differentiating neurons probed with an antibody against Ki-67 and stained with DAPI. 1,000+ cells were counted for each knockdown condition at each time-point after the onset of differentiation. Representative images were counted by four different people, and the average %Ki-67 positive nuclei were plotted here. $N = 1$ for each time-point.....**26**

Figure 2-12. Preliminary investigation into effects of hypervariant loss on NPC proliferation. Quantification of EdU incorporation into dividing neuronal progenitors treated with the nucleoside analog for 1hr. 1000+ cells were counted for each knockdown condition automatically in ImageJ. Relative fluorescence was measured in DAPI positive cells and normalized to background fluorescence of each individual image. Threshold for normalized EdU detection was set at 1. $N = 3$; * represents $p < 0.001$; Mann-Whitney test.....**27**

Figure 2-13. Preliminary investigation into effects of H2A.Z hypervariant loss on cell cycle dynamics in NPCs. A. Example of annotated results of flow cytometry analysis using propidium iodide (PI). B. Representative flow plots from 1 of 2 biological replicates performed in NPCs depleted of either H2A.Z hypervariant and treated with PI. Red boxes highlight apoptotic fraction of each sample; $N = 2$. C. Quantification of PI-stained cells in each phase of the cell cycle and those undergoing apoptosis; $N = 2$**28**

Figure 3-1 Inhibition of translation dysregulates activity-induced expression of Arc, but not via the MAPK pathway. A. Representation of Arc pre-mRNA expression induced by Bic4AP in the presence or absence of translation inhibitors CHX and Anisomycin at different time-points. Expression shown as fold change relative to *Gapdh*. *N* = 5. B, C. Representation of Arc pre-mRNA expression induced by Bic4AP (B) or TTXPMA (C) in the presence of CHX or PD at different time-points. Expression shown as fold change relative to *Gapdh*. D. Western blot showing pERK expression after 60 min treatments with either Bic4AP (D) in the presence of CHX or PD. Error bars represent SEM; * represents $p < 0.05$**34**

Figure 3-2 MAPK pathway is necessary, but not sufficient to induce optimal expression of rapid IEGs. A. Western blot image showing pERK expression after 30 min treatments with TTX and PMA different concentrations. B. Western blot image showing pERK expression induced by TTX and PMA in the presence of different membrane channel inhibitors and PD. C. Representation of pre-mRNA expression levels of rapid IEGs at multiple time-points in response to treatment with Bic/4AP or TTX/PMA; data expressed as fold change relative to *Gapdh* as measured by qPCR; *N* = 3; * represents $p < 0.05$**35**

Figure 3-3 Calcineurin signaling is required for optimal expression of Arc and preventing Calcineurin activation negates the dysregulation of Arc expression induced by inhibition of translation. A. Representation of Arc pre-mRNA levels after induction with Bic/4AP in the presence or absence of CHX and FK-506 at different time-points; data expressed as fold change as measured by qPCR; *N* = 3-5. B. Expression of Arc pre-mRNA levels after induction with Bic/4AP and addition of FK-506 at indicated time-points during the treatment; data expressed as fold change relative to *Gapdh* as measured by qPCR; *N* = 3-5. * represents $p < 0.05$**37**

Figure 3-4 Blocking CaN activation does not affect MAPK signaling. A. Representation of Arc pre-mRNA in response to treatment with TTX and MAPK pathway activators in the presence of PD, FK-506, or both, at different time-points; data expressed as fold change relative to *Gapdh* as measured by qPCR; *N* = 3; * represents $p < 0.05$. B, C. Western blot from whole cell lysates showing effect of FK-506 and PD (or both) on pERK expression in response to treatment with Bic+4AP (B) or TTX+PMA+FSK (C); *N* = 3.....**37**

Figure 3-5 CaN and MAPK pathways are both involved in regulating expression of most rapid IEGs. A. Representation of pre-mRNA levels of rapid IEGs after Bic/4AP treatment with CaN and MAPK inhibitors at different time-points; data represented as fold change relative to *Gapdh* as measured by qPCR; *N* = 3; * represents $p < 0.05$**38**

Figure 3-6 Expression of a fraction of rapid IEGs is regulated by Calcineurin - CRTC1 signaling. A. Western blot image showing CRTC1 expression in nuclear extracts of neurons treated with Bic/4AP for indicated times; *N* = 2. B. Western blot image showing CRTC1 expression in neurons infected with a Scrambled shRNA compared to neurons infected with a CRTC1-specific shRNA; *N* = 2. C. Effect of shRNA-mediated loss of CRTC1 on expression of rapid IEG pre-mRNA in neurons treated with Bic/4AP and collected at different time-points; *N* = 3; * represents *p* < 0.05.....40

Figure 3-7 Calcineurin signaling and CBP HAT domain regulate expression of *Arc* enhancer, SARE. A. Effect of translation inhibition on expression of SARE eRNA in neurons treated with Bic/4AP for 60 min. B. Effect of inhibition of Calcineurin activation on expression of SARE eRNA in neurons treated with Bic/4AP and collected at indicated time-points. C. Representation of SARE eRNA expression in neurons after induction with Bic/4AP and addition of FK-506 at indicated time-points during the treatment. D. Effect of CBP inhibitors on expression of SARE eRNA in neurons treated with Bic/4AP and collected at indicated time-points. For all data sets: *N* = 3-4; * represents *p* < 0.05.....42

Figure 3-8 CBP HAT domain function is necessary for optimal expression of most rapid IEGs. A. Effect of CBP inhibitors on expression of rapid IEG pre-mRNA in neurons treated with Bic/4AP and collected at indicated time-points. Data represented as fold change compared to *Gapdh* as measured by qPCR; *N* = 3; * represents *p* < 0.05.....43

Figure 3-9 Preliminary investigation into the effect of Sik1 depletion on rapid IEG expression. Preliminary representation of rapid IEG pre-mRNA expression in neurons expressing an shRNA specific to Sik1. Cells were treated with Bic+4AP after 5-7 days of infection and collected at different time-points in the presence or absence of FK-506; data represented as fold change relative to *Gapdh*; *N* = 1..45

Figure 4-1 Summary of Findings.....49

LIST OF TABLES

Table 1. List of IEGs expressed in response to neuronal activity and associated brain diseases/disorders.....	3
Table 2. List of histone variants with known roles in regulation of chromatin organization and gene expression.....	6
Table 3. List of point mutations targeted at amino acid differences between H2A.Z.1 and H2A.Z.2.....	20

ACKNOWLEDGEMENTS

I would like to acknowledge the support I have received from colleagues, advisors, and UCM throughout the completion of my dissertation, including my funding sources: UCM's Quantitative and Systems Biology Summer Fellowships and Saha Lab Summer Fellowships.

I would like to acknowledge the significant contribution of ideas (and experimentation in Figure 2-3) made by Pushpita Sarkar and Professor Ramendra Saha in material presented in Chapter 2 of this dissertation, which has been partially adapted from *Dunn, C J et al, 2017*.

I would like to acknowledge that the work presented in this dissertation was made possible by funding from the Saha Lab at UCM.

I would like to thank the members of my committee: Professor Mike Cleary, Professor Masashi Kitazawa, Professor Steve Noctor, and Professor Chris Amemiya for their guidance and flexibility throughout the process of completing the work presented herein.

I would like to extend my gratitude to Professor Katrina Hoyer and Professor Miriam Barlow for their honesty, selfless encouragement, and support throughout my graduate work.

I would like to thank my wonderful undergraduate researchers for their tireless efforts, for making me laugh, and for giving me the opportunity to be a mentor: Natalia Gonzales, Quintin Kuse, Barbara Melo, Joshua Segales, Brenda Gutierrez-Ruiz, Susanna Tejeda-Garibay, Ayna Rejepova, and Mina Ghaninejad-Esfahani.

I would like to thank my colleague, Dr. Robert Poston, for literally always understanding. Enough said.

I would like to extend my deepest gratitude to my best friend, Kristen Valentine, for always being there with a glass of wine, a reality check, or the occasional hug when necessary. Having you by my side through the adventure of graduate school has been an absolute privilege.

ABSTRACT

Recent neurodevelopmental and cognitive studies have described dysregulated expression of immediate early genes (IEGs) as a phenotype and suggest that it may underlie the etiology of increasingly common brain disorders such as Autism and Schizophrenia. Transcription induced by neuronal activity involves the coordinated action of many different processes and factors acting at the membrane, in the cytoplasm, and in the nucleus.

At the chromatin level, one of these factors is the histone variant H2A.Z. While this variant has known roles in memory consolidation and cerebellar development, it has been reported as both a transcriptional activator and repressor. As such, its contribution to transcriptional regulation remains elusive. The work presented here provides evidence supporting distinct roles of H2A.Z hypervariants, H2A.Z.1 and H2A.Z.2, in transcriptional regulation of IEGs and demonstrates a regulatory mechanisms in which the incorporation of H2A.Z.2, not H2A.Z.1, in nucleosomes near the transcription start sites (TSS) of rapid IEGs is required for pausing of RNA Polymerase II (Pol II).

At the cell-signaling level, activity-induced transcription is regulated by multiple calcium-dependent signaling cascades. It has been reported that the Ras/mitogen-activated protein kinase (MAPK) pathway is indispensable for rapid IEG transcription. However, much remains unclear about the involvement of other calcium-dependent signaling cascades in regulating expression of these genes. This study reports evidence supporting the idea that MAPK and Calcineurin (CaN) signaling pathways are both necessary for optimal expression of most rapid IEGs in response to neuronal activity. However, the extent to which each pathway contributes to expression varies from gene to gene.

This study demonstrates variation in the contributions of individual factors (H2A.Z hypervariants) and processes (calcium-induced signaling pathways) to transcriptional regulation. The work herein highlights a need for regulatory mechanisms governing IEG expression to be investigated further at the individual gene level.

Chapter 1: Introduction

1.1 Motivation

IEGs are known to be rapidly transcribed in response to neuronal activity and have been shown to be essential for learning and memory [Gallo et al, 2018]. Many recent neurodevelopmental studies have described dysregulated IEG expression as a phenotype and suggest that it may underlie the etiology of increasingly common brain disorders such as Autism and Schizophrenia [Gallo et al, 2018; Marballi et al, 2018].

Transcription induced by neuronal activity involves the coordinated action of many different processes. Activity sensed at the neuronal membrane must be conveyed to the nucleus via a series of protein interactions known as signaling cascades. When such a signal becomes nuclear, it triggers a series of events that include the activation of transcription factors, DNA-protein interaction, and chromatin re-organization, all of which facilitate gene transcription. As we learn more about the factors involved, it has become clear that not every gene is regulated by the same factors and the function of an individual factor may differ depending on the gene it is involved in transcribing. While much effort has been made toward defining the factors involved in each layer of transcriptional activation, much remains to be understood about the precise function of each factor at the individual gene level.

Understanding the precise set of interactions regulating expression of individual IEGs will contribute to our overall understanding of cognitive disorders and could eventually unlock the ability to develop tools geared toward ameliorating transcriptional dysregulation. It is this goal that provides the motivation for this study.

1.2 Background

1.2.1 *Immediate early genes*

Immediate early genes are a special class of genes transcribed rapidly upon stimulation of neuronal activity, independent of *de novo* protein synthesis. The majority of these genes encode transcription factors, but protein products also include molecules involved in signaling, cellular structure, intracellular transport, and many other processes (refer to Table 1). The first insight describing the potential for neuronal activity-regulated gene transcription came from the discovery that membrane depolarization, and subsequent calcium influx, results in rapid transcription of *c-fos* [Greenberg et al, 1986]. Follow-up work by other groups supported this idea, demonstrating upregulation of *c-fos* and increased Fos expression in different brain regions in response to a variety of sensory stimuli [Hunt et al, 2013; Morgan et al, 1987; Rusak et al, 1990]. Subsequent

studies identified many other genes transcribed in response to neuronal activity [Altar et al 2004; Hong et al, 2004; Li et al, 2004; Nedivi et al, 1993; Park et al, 2006]. Many of these activity-regulated genes encode transcription factors that function to regulate cellular responses to neuronal activity. Others, including brain-derived neurotrophic factor (*Bdnf*) and activity-regulated cytoskeleton associated protein (*Arc*), encode proteins that act locally at the synapse, mediating development and function. Recent reports have defined a subset of IEGs based on a shared regulatory mechanism wherein Pol II is pre-bound near the transcription start site TSS, termed Pol II pausing [Saha et al, 2011]. IEGs regulated by Pol II pausing are called rapid IEGs. A striking amount of evidence links dysregulated expression of rapid IEGs to neurodevelopmental disorders (see Table 1) and necessitates a complete understanding of the molecular dynamics governing transcription of these genes in the brain.

1.2.2 Nucleosomal regulation of transcription: the role of histone variants

Activity-induced gene transcription is regulated at the chromatin level by the ability of transcription machinery to access DNA [Greer and Greenberg, 2008]. Several activity-induced neuronal IEGs are accessed independent of signal by a pre-bound Pol II that pauses proximal to the promoter until an activity signal is received [Saha et al, 2011, Adelman et al, 2012]. Nucleosomes, the fundamental chromatin unit, regulate Pol II elongation by acting as either barriers or facilitators [Owen-Hughes, 2012; Teves et al, 2014]. Functional differences of nucleosomes arise from histone tail modifications and the incorporation of variant histones [Michod et al, 2012].

In mammals, three of the four canonical histones, H2A, H2B, and H3, have diversified into multiple variant histones, each having distinct amino acid sequences that can influence nucleosomal properties and dynamics, thus differentially affecting transcription (see Table 2) [Weber and Henikoff, 2018; Biterge and Schneider, 2014; Doyen et al, 2006; Talbert et al, 2017; Tolstorukov et al, 2012; Zhen et al, 2019]. Some studies have highlighted important roles of histone variants H2A.Z and H3.3 in neuronal gene transcription underlying brain development and function. For example, it has been reported that H2A.Z, which shares about 60% sequence similarity to canonical H2A and is conserved from yeast to human, plays a role in memory consolidation and cerebellar development in the brain [Zovkic et al, 2014; Yang et al, 2016]. Interestingly, H2A.Z has been implicated in both transcriptional activation and repression [Soboleva et al, 2014]. This discrepancy, combined with characterization of two functionally non-redundant variant isoforms, H2A.Z.1 and H2A.Z.2, necessitates further investigation into the molecular dynamics underlying this variant's contribution to transcriptional regulation.

Table 1. List of IEGs expressed in response to neuronal activity and associated brain diseases/disorders.

Gene	Rapid or Delayed	Encoded protein type/function	Disease/disorder association	Expression phenotype
Fosb	R	TF	ASD	down
Npas4	R	TF	memory, schizophrenia, emotional impairments, ASD	down
cFos	R	TF	schizophrenia	
Junb	R	TF		
Nr4a1 (Nur77)	R	TF	schizophrenia	down
Egr4	R	TF	schizophrenia	down
Arc	R	Cytoskeletal signaling	schizophrenia, ASD, ID, Rett Syndrome, depression	up/down
Egr2	R	TF	schizophrenia, Rett syndrome, ASD	up
Zif268 (Egr1)	R	TF	memory, schizophrenia	up
Maff	R	TF		
Ier2	R	TF		
Klf4	R	TF	schizophrenia, ASD	down
Dusp1	R	MAPK phosphatase		
Gadd45g	R	stress response factor	memory deficits	down
Dusp5	R	MAPK phosphatase		
Egr3	R	TF	schizophrenia, autism, bipolar disorder	down
Btg2	R	TF	schizophrenia	down
Pppr1r15a	R	stress response factor		
Amigo3	R	signal transduction		
Arf4	R	signal transduction		
Cyr61 (Ccn1)	R	intercellular adhesion	schizophrenia	up
Dusp6	R	MAPK phosphatase	schizophrenia, bipolar disorder	down
Gadd45b	R	stress response factor		
Nr4a3	R	TF	schizophrenia	down
Nup98	D	nuclear pore factor		
Pcsk1	D	intracellular trafficking		
Col10a1	D	intracellular signaling		
Bdnf	D	intracellular signaling		
Klf14	D	TF		
C2cd4b	D	intercellular adhesion		
Cartpt	D	stress response factor		
Gprc5a	D	G-protein coupled receptor		
Gch1	D	calcium binding		
Pax1	D	TF		

Scg2	D	vesicle packaging	
Crem	D	TF	
Cort	D	cellular signaling	
Ptger4	D	G-protein coupled receptor	
Sertad1	D	TF	
Csmp1	D	TF	
Rgs2	D	GTPase activator	
Crhbp	D	peptide binding	
Adcyap1	D	signal transduction	
Fosl2	D	TF	
Rel	D	TF	
Zdbf2	D	nucleic acid binding	
Prok2	D	GPCR binding	
Areg	D	vesicle transport	
Grasp	D	neuronal molecular scaffold	
Ptgs2 (Cox2)	D	lipid binding	
Sult2b1	D	sulfotransferase activity	
Nppc	D	hormone activity	
Tacr3	D	GPCR activity	
Gpr22	D	GPCR activity	
Pcdh8	D	calcium ion binding	
Bves	D	cAMP binding	
Chrm2	D	GPCR activity	
Kitl	D	cytokine activity	
Tac1	D	hormone activity	
Nrn1	D	neurite outgrowth/arborization	
Nefl	D	intracellular transport	
Pou3f1	D	TF	
Eil2	D	TF	
Errfi1	D	protein kinase binding	gliomas
Mthfd2	D	magnesium ion binding	
Rgs4	D	GTPase activator, MEK-ERK pathway activator	schizophrenia, psychotic disorder
Lipg	D	phospholipase activity	
Nr4a2 (Nurr1)	D	TF	dopaminergic dysfunction, schizophrenia, manic depression
Kcnj3	D	inward rectifier potassium channel	
Slc2a3	D	transmembrane transporter	
Rem2	D	GTPase activity	

Per1	D	TF	sleep disorders	
Atf3	D	TF	neuropathy	
Mam13	D	transcription coactivator		
Mctp2	D	calcium ion binding		
Gpr26	D	GPCR activity	neurodegenerative disorders	
Per2	D	TF	sleep disorders	
Tbc1d8b	D	GTPase activator		
Plagl1	D	TF	neonatal diabetes	
Peg10	D	TF		
Sv2c	D	transmembrane transporter		
Chml	D	GTPase activator		
Adm	D	signaling molecule		
Sik1	D	protein tyrosine kinase activity	epileptic encephalopathy	
Hctr2	D	GPCR activity	Sleep disorder	
Rasgrp1	D	calcium ion binding		
Pgap1	D	hydrolase activity	intellectual deficiency	
Pard6a	D	TF		
Dusp14	D	MAPK phosphatase		
Rheb	D	GTP binding		
Stard4	D	lipid binding		
Gmeb2	D	transcription coactivator		
Dusp4	D	MAPK phosphatase		
Fam46a	D	nucleotidyltransferase	Posterior Cortical Atrophy	
Gem	D	GTP binding		
Herpud1	D	ion channel binding		
Eprs	D	aminoacyl-tRNA synthetase	Microcephaly, seizures, cerebellar atrophy	
Slc6a17	D	transporter	intellectual disability	
Mpp7	D	guanylate kinase		
Acsl4	D	ligase	intellectual disability	
Hsd17b12	D	dehydrogenase		
Spty2d1	D	histone chaperone		
Slc7a1	D	transmembrane transporter		
Ccno	D	uracil DNA glycosylase		
Edn1	D	signaling receptor binding		
Egr3	D	TF		
Fam46b	D	nucleotidyltransferase		
Fosl1	D	TF		
Ifng	D	type II interferon		
Nfil3	D	TF		

Ras11a	D	GTPase	
Sgk1	D	serine/threonine kinase	
Trib1	D	TF	
Vgf	D	growth factor	

Table 2. Histone variants with known roles in regulation of chromatin organization and gene expression.

Histone	Known Functions
H2A	canonical
H2A.B.2/H2A.Bbd	Nucleosome destabilization, active transcription
H2A.B.3	Post-transcriptional RNA processing
macroH2A	X chromosome inactivation
H2A.X	DNA double strand break repair
H2A.Z.1	Active transcription, development
H2A.Z.2	Active transcription, DNA repair
H3	canonical
cenH3-CENPA	Centromere stability, kinetochore complex recruitment
H3.3	Transcription activation

1.2.3 Activity-induced signaling pathways in the brain

Neuronal activity results in increased concentrations of intracellular calcium. Calcium can enter the cell via voltage-gated calcium channels or ligand-gated ion channels [Berridge, 1998; Jonas et al, 1995], and resulting gene induction patterns vary depending on the mode of entry [Bading, 1993; Ghosh et al, 1994; Ginty et al, 1997; Westenbroek et al, 1992]. Well-known calcium-dependent transcription regulators include the calcium/calmodulin-dependent protein kinases (CaMKs), the serine/threonine protein phosphatase CaN, and MAPKs. The activation of these proteins by intracellular calcium triggers signaling cascades (either a series of phosphorylation or dephosphorylation reactions) that convey patterns of membrane depolarization to the nucleus. Each pathway has specific downstream effectors that are imported into the nucleus and function to regulate gene transcription.

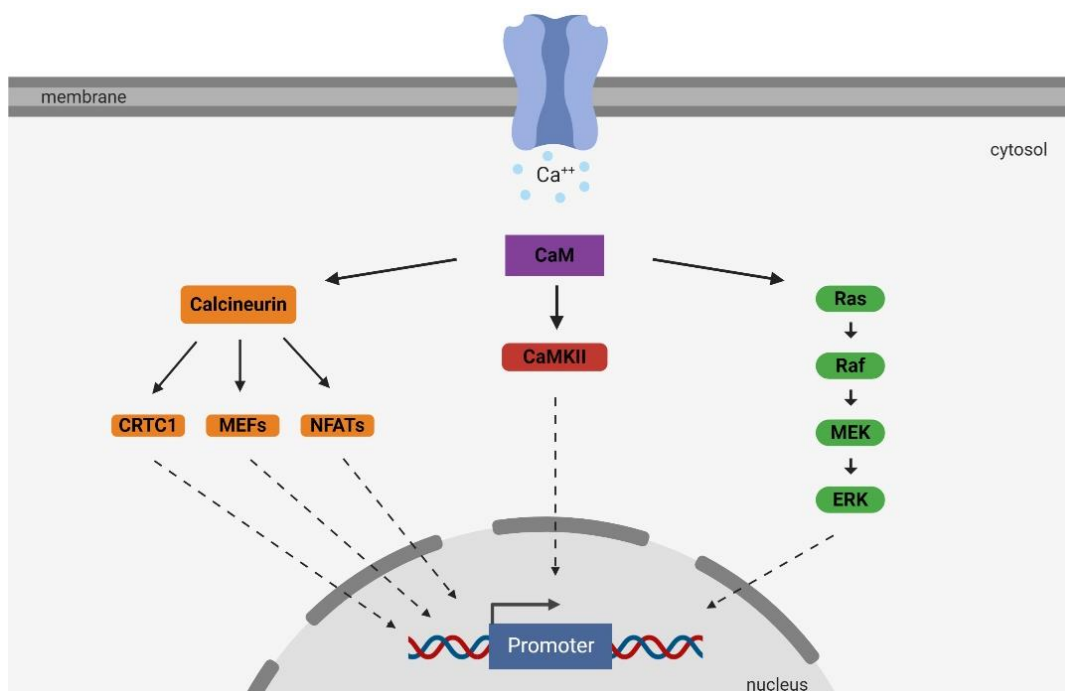


Figure 1-1. Calcium-dependent signaling pathways regulating activity-induced gene transcription in the brain.

Recent reports have defined IEG subsets based on shared regulatory mechanisms [Saha et al, 2011] and shown that activation of the calcium-dependent MAPK pathway is required for rapid recruitment of Pol II to rapid IEG promoters [Tyssowski et al, 2018]. However, it is known that a handful of well-characterized IEGs are differentially regulated by distinct modes of activity-induced calcium entry. For example, transcription of *bdnf* is rapidly induced in response to calcium entry through L-type voltage-sensitive calcium channels (VSCCs) specifically [Ghosh et al, 1994; Westenbroek et al, 1992]. This

highlights the fact that individual IEGs may be regulated by unique mechanisms. Therefore, a complete understanding of activity-induced gene expression in the brain will require that regulatory mechanisms governing IEG transcription be studied at the individual gene level.

The work presented in this dissertation contributes to our overall understanding of how individual IEGs are regulated by variant H2A.Z, as well as how rapid IEGs are regulated by different calcium-dependent signaling cascades.

Chapter 2: Regulation of Neuronal Immediate-early Gene Transcription by H2A.Z Hypervariants

2.1 Introduction

Activity-induced gene transcription, an integral component of neural plasticity, is conducted at the chromatin level by enabling the transcription machinery to access and “read-out” DNA [Greer and Greenberg, 2008]. Several activity-induced neuronal immediate early genes (IEGs) are accessed independent of signal by a transcriptionally engaged Pol II that pauses proximal to the promoter until an activity signal is received [Adelman et al, 2012, Saha et al, 2011]. Activity-induced signals release the paused Pol II, which then transcribes the gene by running through spools of nucleosomes (productive elongation). Nucleosomes, the fundamental chromatin unit, regulate Pol II elongation by acting as either barriers or facilitators [Owen-Hughes, 2012; Teves et al, 2014]. Such activity-dependent nucleosomal role selection primarily depends on post-translational modifications of the histone tails and nucleosomal remodeling, including turnover of different histone variants [Michod et al, 2012].

In mammals, three of the four canonical histones, H2A, H2B, and H3, have diversified into several variant histones with distinct amino acid sequences that can influence the dynamics of transcription [Weber and Henikoff, 2018]. Recently, a few studies have unveiled important roles of histone variants H2A.Z and H3.3 in neuronal gene transcription underlying brain development and function. For example, H2A.Z, which is conserved from yeast to human and has been implicated in both transcriptional activation and repression [Soboleva et al, 2014], plays a role in memory consolidation and cerebellar development in the brain [Yang et al, 2016; Zovkic et al, 2014]. Similarly, H3.3, which differs from canonical H3 histones by only four to five amino acids [Filipescu et al, 2013], regulates embryonic and adult neuronal gene expression patterns, thereby playing an essential role in plasticity and cognition [Maze et al, 2015]. This example illustrates how very small differences in the sequences of two closely related histone proteins may result in differential regulation of neuronal gene transcription [Maze et al, 2014].

Similar small differences exist within the H2A.Z histone class. In vertebrates, H2A.Z has two very closely related paralogs that have been referred to as ‘hypervariants’: H2A.Z.1 (formerly H2A.Z) and H2A.Z.2 (formerly H2A.V) [Talbert et al, 2012]. These hypervariants are encoded by two nonallelic genes, *H2afz* and *H2afv*, which are driven by independent promoters on different chromosomes [Dryhurst et al, 2009; Matsuda et al, 2010]. H2A.Z.1 and H2A.Z.2 differ by only three amino acids (see Figure 2-1), which are located far apart on the polypeptide and are structurally similar to their respective counterpart in that there are no usable differences in their antigenicity (e.g., hydrophobic vs hydrophilic, ring structure vs linear, or large vs small in residue size). Thus, there

are currently no antibodies available to distinguish between H2A.Z.1 and H2A.Z.2. Due to this limitation, our understanding of H2A.Z is most likely based on a combination of both hypervariant phenotypes. Such a composite picture of their function would not be a concern if these hypervariants were functionally redundant and homogeneous [Soboleva et al, 2014].

```

H2A.Z.1  AGGKA GKDSG KAKTK AVSRS QRAGL QFPVG RIHRH LKSR...V L E L A G N A...KTV
          1     6     11    16     21     26     31     36     66     126
H2A.Z.2  AGGKA GKDSG KAKAK AVSRS QRAGL QFPVG RIHRH LKTR...V L E L A G N A...KTA

```

Figure 2-1. Amino acid differences between H2A.Z.1 and H2A.Z.2.

However, a few structural and functional features suggest the contrary. Recently resolved crystal structures of H2A.Z-containing nucleosomes revealed subtle differences in the H2A.Z.1 and H2A.Z.2 L1 loop [Horikoshi et al, 2013], but it remains unknown whether such differences manifest any functional consequences. In H2A.Z.1^{-/-} mice, which are embryonic lethal [Faast et al, 2001], H2A.Z.2 is apparently unable to compensate for the loss of its twin isoform, thereby suggesting a unique role for H2A.Z.1 during early embryonic development. Similar functional inequality of H2A.Z.1 and H2A.Z.2 has also been recently reported in melanoma cells [Vardabasso et al, 2015]. Taken together, there remains an untested possibility that these two H2A.Z hypervariants may not be functionally identical, but instead have discrete roles (functional specificity) in gene transcription. This hypothesis was tested in neurons and we observed that H2A.Z.1 and H2A.Z.2 have independent and context-specific roles in basal and neuronal activity-induced gene transcription.

2.2 Results

2.2.1 H2A.Z.1 and H2A.Z.2 play gene- and context-specific roles in regulating activity-induced transcription of rapid immediate early genes

To study the effects of H2A.Z hypervariant depletion on rapid IEGs, activity was induced in neurons under two different biological contexts. In resting neurons, neuronal activity was stimulated in dissociated neurons by blocking inhibitory GABA_A receptors (using Bic) and simultaneously blocking K⁺ channels (using 4AP), resulting in increased burst frequency (Bic+4AP) [Papadia et al, 2005]. To induce a homeostatic change, the TTX washout assay [Rao et al, 2006; Saha et al, 2011] was used. This assay involves treating neurons with TTX for 48 h to induce homeostatic synaptic changes, followed by TTX washout to trigger rapid and robust network activity that induces gene transcription. Using these methods to induce activity in different neuronal contexts, we assessed expression of a handful of genes identified in a previous study [Saha et al, 2011] in the absence of either H2A.Z hypervariant (Figure 2-2 A). In general, gene expression was amplified in cells that had undergone homeostatic changes prior to induction of activity, which was expected. Many of the genes examined maintained similar

temporal expression dynamics under both biological contexts. However, while expression of some genes was sensitive to depletion of both hypervariants, all genes examined were more dramatically affected by depletion of H2A.Z.2 compared to H2A.Z.1. To investigate this further, we looked at the effect of hypervariant depletion on expression of all rapid IEGs (identified in a previous study [Saha et al, 2011]) under both biological contexts using a multiplexed gene expression analysis called NanoString. Notably, the results of the NanoString analysis (Figure 2-2 B, D, E) were consistent with the qPCR analysis done in-house (Figure 2-2 A). This expanded gene expression data supports the notion that rapid IEG expression is more dramatically affected by loss of H2A.Z.2 than

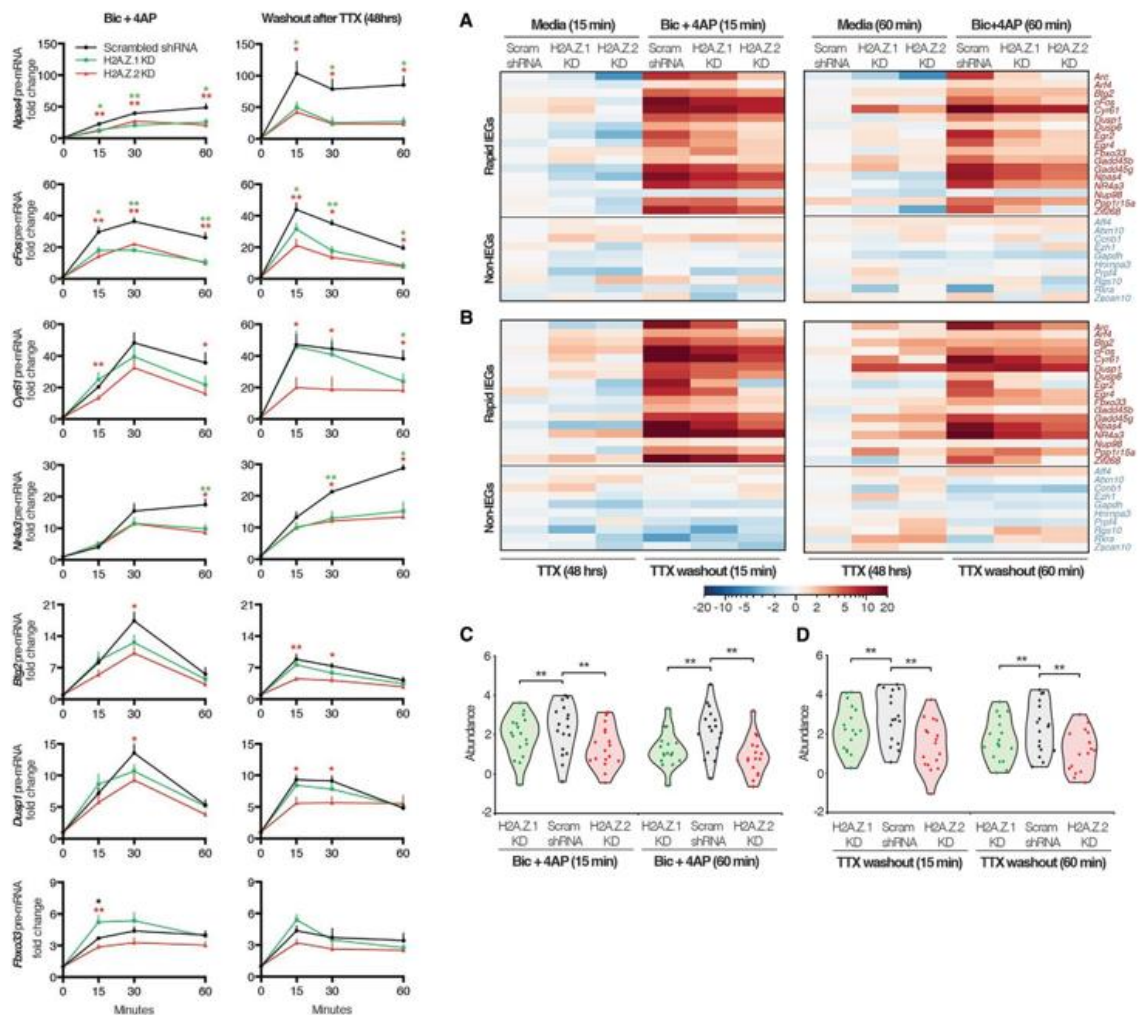


Figure 2-2. H2A.Z.1 and H2A.Z.2 play context-dependent roles in activity-induced transcription of rapid IEGs. (A) Representation of pre-mRNA levels for noted IEGs at different time-points after two treatment regimens. *Left*, Bic+4AP treatment. *Right*, 48hr treatment with TTX followed by its washout for specified time periods in indicated groups of neurons as detected by qPCR and normalized to *Gapdh*. $N = 4-7$ for each time-point. (B) Nanostring multiplexed gene expression data (heat maps) representing pre-mRNA levels in control and hypervariant-depleted neurons treated with Bic+4AP for indicated times. (C) Heat maps representing pre-mRNA levels in control and hypervariant-depleted neurons treated with TTX for 48hr followed by washout for indicated times. $N = 3$ for each treatment at all time-points. * $p < 0.05$ and ** < 0.01 (Wilcoxon paired non-parametric test).

H2A.Z.1. Overall, it appears as though loss of H2A.Z hypervariants results in decreased expression of rapid IEGs, regardless of cellular state, and that individual hypervariants may have gene- and context-specific roles in regulating transcription of rapid IEGs.

2.2.2 H2A.Z hypervariant-specific RNAi has differential effects on activity-induced transcription of Arc

To study the role(s) of H2A.Z hypervariants on transcriptional regulation of a model gene, we chose to investigate the rapid IEG *Arc*, which responds quickly to neuronal activity [Guzowski et al, 1999; Saha et al, 2011]. *Arc* was chosen for several reasons: (1) it is a neuron-specific IEG, which has been extensively studied previously by us and others, (2) its promoter and TSS regions are enriched with H2A.Z-containing nucleosomes (our unpublished observations), and (3) it is one of the genes shown to be regulated by H2A.Z in cognitive functions [Zovkic et al, 2014]. Using the Bic+4AP protocol, we induced gene transcription and evaluated *Arc* mRNA abundance at 15 min after treatment.

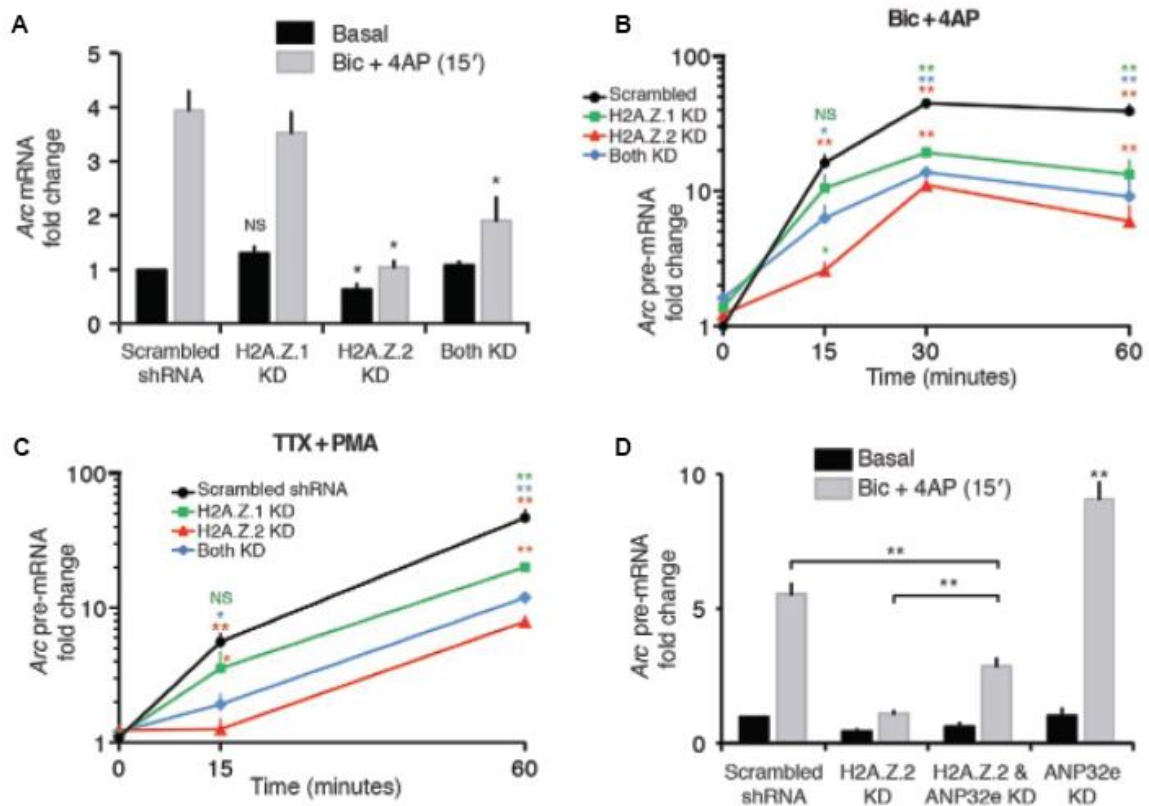


Figure 2-3. H2A.Z hypervariant-specific RNAi has differential effects on activity-induced transcription of Arc. A. Representation of Arc mRNA level at 15 min after treatment with Bic+4AP in indicated neuronal groups as detected by qPCR and normalized to *Gapdh*. $N = 3-4$ for each group. B, C. Representation of Arc pre-mRNA level at different time points after treatment with Bic+4AP (B) or TTX+PMA (C) in indicated groups of neurons (5–6 d postinfection) as detected by qPCR and normalized to *Gapdh*. $N = 3-4$ for each time point. D. Representation of Arc pre-mRNA level at 15 min after treatment with Bic+4AP in indicated neuronal groups as detected by qPCR and normalized to *Gapdh*. $N = 3$. For all figures, * $p < 0.05$; ** $p < 0.01$; NS, not significant

Basal and induced *Arc* mRNA levels were unaffected by H2A.Z.1 depletion but were significantly diminished in H2A.Z.2-depleted cells (Figure 2-3 A).

Because mRNA abundance is not necessarily a reflection of transcription per se but rather the net result of both synthesis and decay rates, we next evaluated *Arc* pre-mRNA, as it is the direct readout of transcription [Wu et al, 2012]. We detected no significant differences in the basal level of *Arc* pre-mRNA with H2A.Z hypervariant depletions (Figure 2-3 B, 0-min time-point). After Bic+4AP treatment, *Arc* pre-mRNA levels increased significantly within 15 min and continued to increase with time in control neurons. However, in agreement with the mRNA data (Figure 2-3 A), the pre-mRNA response in H2A.Z.2-depleted neurons was attenuated at the early time point (15 min) and was also significantly reduced at later points (Figure 2-3 B). In contrast, H2A.Z.1 depletion had no effect on *Arc* pre-mRNA levels at 15 min. However, at later time points, H2A.Z.1-depleted neurons had significantly less *Arc* pre-mRNA than control neurons but had significantly more than in neurons depleted of H2A.Z.2 (Figure 2-3 B). These results suggest that although the loss of H2A.Z.1 impaired *Arc* transcription significantly at later time points, loss of H2A.Z.2 had a much stronger effect at all time points. Unexpectedly, we did not observe a combined effect on pre-mRNA expression when both hypervariants were depleted. While trying to knockdown both H2A.Z.1 and H2A.Z.2, we had to titer our viral infection and infect with less of each virus to avoid causing cell death due to viral overload. Therefore, less knockdown (KD) was achieved in the dual KD cells compared to their single KD counterparts. Such reduced knockdown may explain the intermediate effect of knocking down both H2A.Z.1 and H2A.Z.2 on *Arc* transcription. In support of these observations, hypervariant-specific effects on activity-induced ARC protein abundance were generally reflective of *Arc* pre-mRNA expression patterns [Dunn et al, 2017].

Because some synaptic alterations were noted due to H2A.Z hypervariant depletion [Dunn et al, 2017] and because Bic+4AP treatment is a synapse-dependent activity induction protocol, we next tried to induce *Arc* expression extrasynaptically by jump-starting the MAPK pathway intracellularly [Rosen et al, 1994; Wiegert et al, 2011]. The MAPK pathway was extrasynaptically activated via PKC using PMA [Schultz et al, 1998] in the presence of TTX to prevent any synaptic input, and this treatment induced rapid transcription of *Arc* (Figure 2-3 C). When H2A.Z hypervariant-depleted neurons were stimulated using this protocol, the outcome was similar to what was seen with the Bic+4AP protocol (Figure 2-3 B). These observations suggest that effects of H2A.Z hypervariant depletion on activity-induced *Arc* transcription are most likely not limited to effects of changing synaptic components. Supporting this assertion is the observation that H2A.Z hypervariant depletion had no effect on activity-induced activation of the MAPK pathway as indicated by 12hosphor-ERK1/2 levels [Dunn et al, 2017].

To further test the specificity of the H2A.Z.2 depletion-induced phenotype, we attempted to rescue *Arc* induction by combining shRNA-mediated knockdown

with co-expression of shRNA-insensitive H2A.Z.2 (Myc-H2A.Z.2-IS) [Dunn et al, 2017]. Several such experimental designs were unsuccessful, likely due to a lack of regulatory post-translational modifications on exogenous constructs in the absence of endogenous proteins and/or perturbation of a critical balance of endogenous levels of these hypervariants and their chaperones. A recent report demonstrated that loss of phenotype due to depletion of an H2A.Z chaperone (ANP32E) could be rescued by co-depletion of ANP32E and H2A.Z [Alatwi et al, 2015]. Accordingly, we co-depleted ANP32E ($92.0 \pm 0.1\%$ knockdown on day 5 after infection) with H2A.Z.2 and observed a partial rescue of *Arc* transcription (Figure 2-3 D). Taken together, our data show non-redundant roles of H2A.Z hypervariants in the regulation of *Arc* transcription and hint at the importance of a fine balance between histones and their chaperones in mediating such responses.

2.2.3 H2A.Z.2 facilitates priming of the *Arc* promoter

It has been shown that H2A.Z is enriched near the TSS of *Arc* [Zovkic et al, 2014]. To study the underlying mechanism of H2A.Z.2's role in rapid *Arc* transcription, we tested the effect of its knockdown on histone acetylation and promoter proximal RNA Pol II pausing based on recent reports [Saha et al, 2011; Vardabasso et al, 2015]. In melanoma cells, knockdown of H2A.Z.2, but not H2A.Z.1, attenuates acetylation of histone H3 and H4 globally [Vardabasso et al, 2015]. While we did not observe similar effects of H2A.Z.2 depletion on H3 or H4 acetylation in neurons (data not shown), this difference could be due to cell-type-specific phenomena relevant to dividing cells. Instead, we noted that H2A.Z.2 depletion led to a decrease in Ac-H2A.Z levels globally (Figure 2-4 A) and near the *Arc* TSS (Figure 2-4 B, C). Note that the data presented in Figure 2-4 C are normalized by total H2A.Z, the level of which remained unaltered after

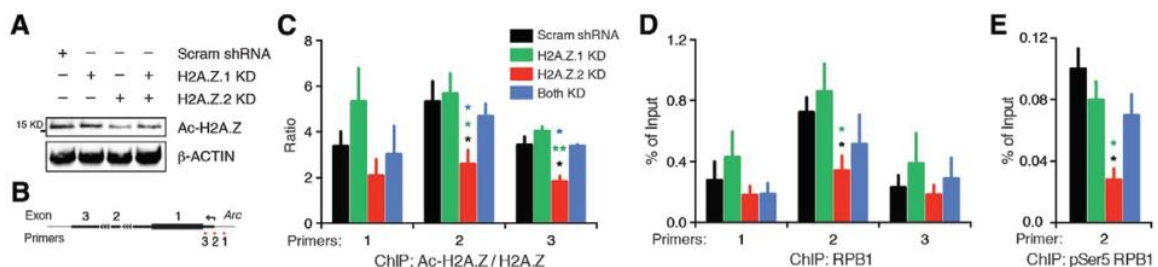


Figure 2-4 H2A.Z.2 facilitates priming of the *Arc* promoter. A. Representative Western blotting of whole-cell lysate showing Ac-H2A.Z levels in neurons depleted of H2A.Z hypervariants as indicated. $N = 3$. B. Graphical map (not to scale) depicting relative position of ChIP primers near *Arc* TSS. C. Quantification of Ac-H2A.Z (normalized by total H2A.Z) binding to *Arc* TSS region in neurons treated as indicated, determined by ChIP. $N = 4$. Two sets of data in statistical comparison are represented by the position and the color of asterisk(s). D. ChIP data demonstrating binding of RPB1 to the *Arc* TSS region in control neurons or H2A.Z hypervariant-depleted neurons as indicated. $N = 4$. E. ChIP data demonstrating binding of pSer5-RPB1 to the *Arc* TSS in control and hypervariant-depleted neurons. $N = 3$. * $p < 0.05$ and ** $p < 0.01$

hypervariant knockdown. The effect was not mimicked by H2A.Z.1 depletion. This suggests that H2A.Z.2 depletion results in selective loss of acetylation, not total H2A.Z, near the TSS of *Arc*. Presence of TSS proximal H2A.Z highly correlates with another chief component of rapid IEG transcription, RNA Pol II pausing [Day et al, 2016]. It has been shown that RNA Pol II is loaded and paused near TSS of *Arc* and other rapidly induced IEGs, and underlies the ability of these genes to respond to activity within a few minutes [Saha et al, 2011]. Here, we tested whether there is a relation between Pol II pausing and H2A.Z hypervariants at the *Arc* TSS. Using ChIP with an antibody against RPB1 (N-terminus), the largest Pol II subunit, we found that RNA Pol II pausing at the *Arc* TSS is diminished significantly in neurons depleted of H2A.Z.2, but not H2A.Z.1. While it is unlikely that our anti-RPB1 antibody precipitates nonspecific proteins or is less efficient after hypervariant depletion, we sought to corroborate our findings with another antibody to further ensure that H2A.Z.2 depletion was affecting paused Pol II. We performed ChIP with an antibody specific to RPB1 phosphorylated at serine 5 (pSer5) residue of C-terminal domain heptad repeats. pSer5-RPB1 represents the pool of RPB1 that is transcriptionally engaged but has not entered productive elongation (paused). Our data indicate that actively engaged Pol II at the +1 nucleosome of *Arc* is significantly reduced by the loss of H2A.Z.2, but not H2A.Z.1 (Figure 2-4 C). This hypervariant-specific loss of Pol II pausing provides an explanation for our observations at 15-min post-Bic + 4AP treatment (Figure 2-3 B) where *Arc* pre-mRNA levels were minimal in H2A.Z.2-, but not in H2A.Z.1-, depleted neurons.

2.2.4 *H2A.Z.1 plays context-dependent roles in Arc transcription*

To determine a potential role for H2A.Z.1 in *Arc* transcription, we hypothesized that it may facilitate Pol II recruitment or elongation during active transcription. To test these possibilities, *Arc* transcription was induced using the DRB washout protocol with or without Triptolide (Trip). DRB is a nucleoside analog that inhibits mammalian transcription by interfering with the DRB sensitivity-inducing factor (DSIF) complex that enables RNA Pol II pausing in the presence of negative elongation factor (NELF), and then facilitates productive elongation once NELF falls off in response to external signals [Kwak et al, 2013]. Because DRB can be washed out, DRB washout assays have been used to achieve rapid and synchronized transcription elongation without additional extranuclear signals [Lee et al, 2015]. When control neurons were subjected to this assay, we observed a rapid and robust *Arc* induction (Figure 2-5 A). DRB washout resulted in significant upregulation of *Arc* pre-mRNA levels within three minutes, which then continued to increase over time to reach >100-fold at 15 min. Depletion of H2A.Z.2 resulted in, as we saw with Bic + 4AP and TTX + PMA assays, an attenuated response at the early time-point that partially recovered at later time points, but remained significantly less than the normal response (Figure 2-5 A).

In contrast, depletion of H2A.Z.1 had no effect on DRB washout-triggered *Arc* transcription (Figure 2-5 A), indicating that H2A.Z.1 is likely not involved in the productive elongation phase.

Next, to test for any role of H2A.Z in RNA Pol II recruitment, a phenomenon that sustains robust responses by providing the gene promoter with a chain of Pol II complexes, DRB was washed out in the presence of Trip, a diterpene triepoxide isolated from natural sources. Trip inhibits Pol II recruitment to promoters by inhibiting TFIID, the pre-initiation complex component that mediates Pol II binding to DNA [Titov et al, 2011]. When DRB washout was performed in the presence of a low concentration of Trip, *Arc* transcription was significantly reduced at later time points (Figure 2-5 A) suggesting that the slightest interference with Pol II

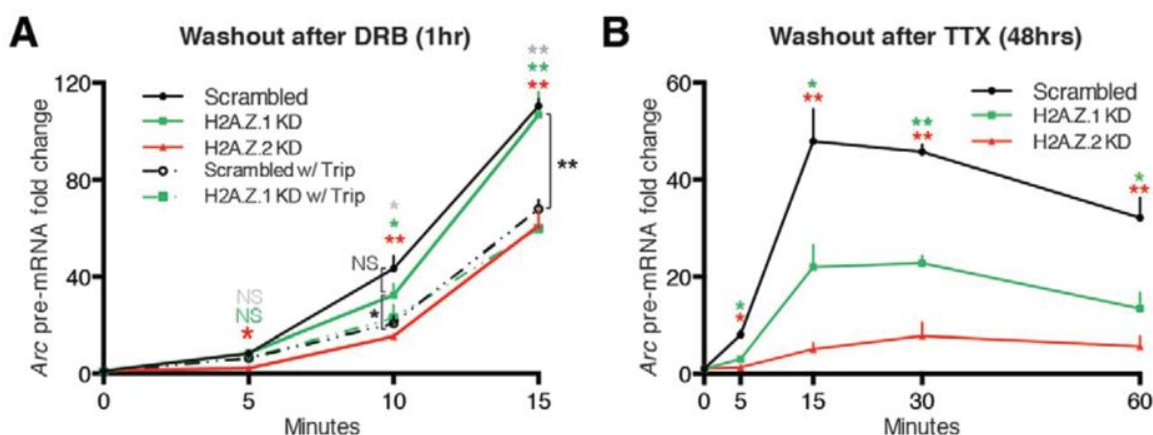


Figure 2-5 H2A.Z.1 plays context-dependent roles in *Arc* transcription. A. Graphical representation of the level of *Arc* pre-mRNA at different time points after 1-h treatment with DRB (5,6-dichloro-1-beta-D-ribofuranosylbenzimidazole) followed by its washout for indicated time periods in the presence or absence of Trip in indicated groups of neurons (infected for 5–6 d) as detected by qPCR and normalized to Rn18s (18s rRNA; DRB inhibition-insensitive, Pol III-dependent transcription). Gray, green and red asterisk(s) or NS represent statistical comparison between control (Scrambled) responses and responses in Scrambled w/Trip, H2A.Z.1 KD w/Trip and H2A.Z.2 KD, respectively. Connecting brackets delineate other comparisons, shown in black asterisk(s) or NS. B. Similar dataset as in (A) except that control neurons or hypervariant-depleted neurons were treated with TTX for 48 h followed by its washout for indicated time periods. Two sets of data in statistical comparison are represented by the position and the color of asterisk(s) or NS. For both A, B. $N = 4-5$ for each time point; * $p < 0.05$ and ** $p < 0.01$. NS, not significant

recruitment compromises the robustness of the response. Had H2A.Z.1 played a role in Pol II recruitment, its depletion would have had an effect comparable to washout with Trip in control cells. However, that does not seem to be the case as the *Arc* response is significantly different between these two groups. Moreover, control and H2A.Z.1-depleted neurons responded similarly to induction in the presence of Trip suggesting that H2A.Z.1 is unlikely to be required for Pol II recruitment.

To test the roles of H2A.Z hypervariants in another neurobiological context, we next performed the TTX washout assay (Figure 2-5 B). Consistent with other induction assays so far, H2A.Z.2 depletion had an attenuating effect on early

transcriptional response, followed by partial recovery at later time points (Figure 2-5 B). Surprisingly, depletion of H2A.Z.1 significantly reduced the *Arc* response throughout, even the early time points. This is in contrast with the insensitivity of the *Arc* response at early time points in all induction assays, including 15-min postinduction with Bic + 4AP under resting (control) conditions. Together, our data suggest that H2A.Z.1 exerts context-dependent effects on activity-induced *Arc* transcription.

2.2.5 H2A.Z hypervariants are involved in regulating transcription of delayed IEGs in neurons

Because we saw gene-to-gene variation in H2A.Z hypervariant regulation of rapid IEG transcription, we asked if these hypervariants might also be involved in regulating transcription of another class of IEGs, referred to as delayed IEGs [Saha et al, 2011]. Based on the lack of a role for paused Pol II in the delayed IEG transcription [Saha et al, 2011], we expected to find no effect of hypervariant depletion. However, we found a context-dependent regulation of delayed IEGs, and some trends are noted in the following lines: at 60-min postinduction, depletion of H2A.Z.1 appears to result in downregulation of *Cox2*, *Klf4*, and *Nur77* with Bic + 4AP induction, but

results in upregulation of the same genes on induction after TTX-induced changes. Differential regulation between neurobiological contexts was also evident after loss of H2A.Z.2 in *Cartpt* and *Fam46a* (Figure 2-6 A). Interestingly, group statistical comparisons of delayed IEG responses in hypervariant-depleted neurons to control neurons show that loss of H2A.Z.1 only has a significant effect at the early time-point on induction after 48 h of TTX. However, upon induction in resting neurons (Bic + 4AP assays), H2A.Z.1 depletion only significantly affects the group at the late time point (Figure 2-6 B). Overall, these data suggest that the roles of H2A.Z hypervariants in regulating transcription of delayed IEGs may vary depending on specific genes and cellular states.

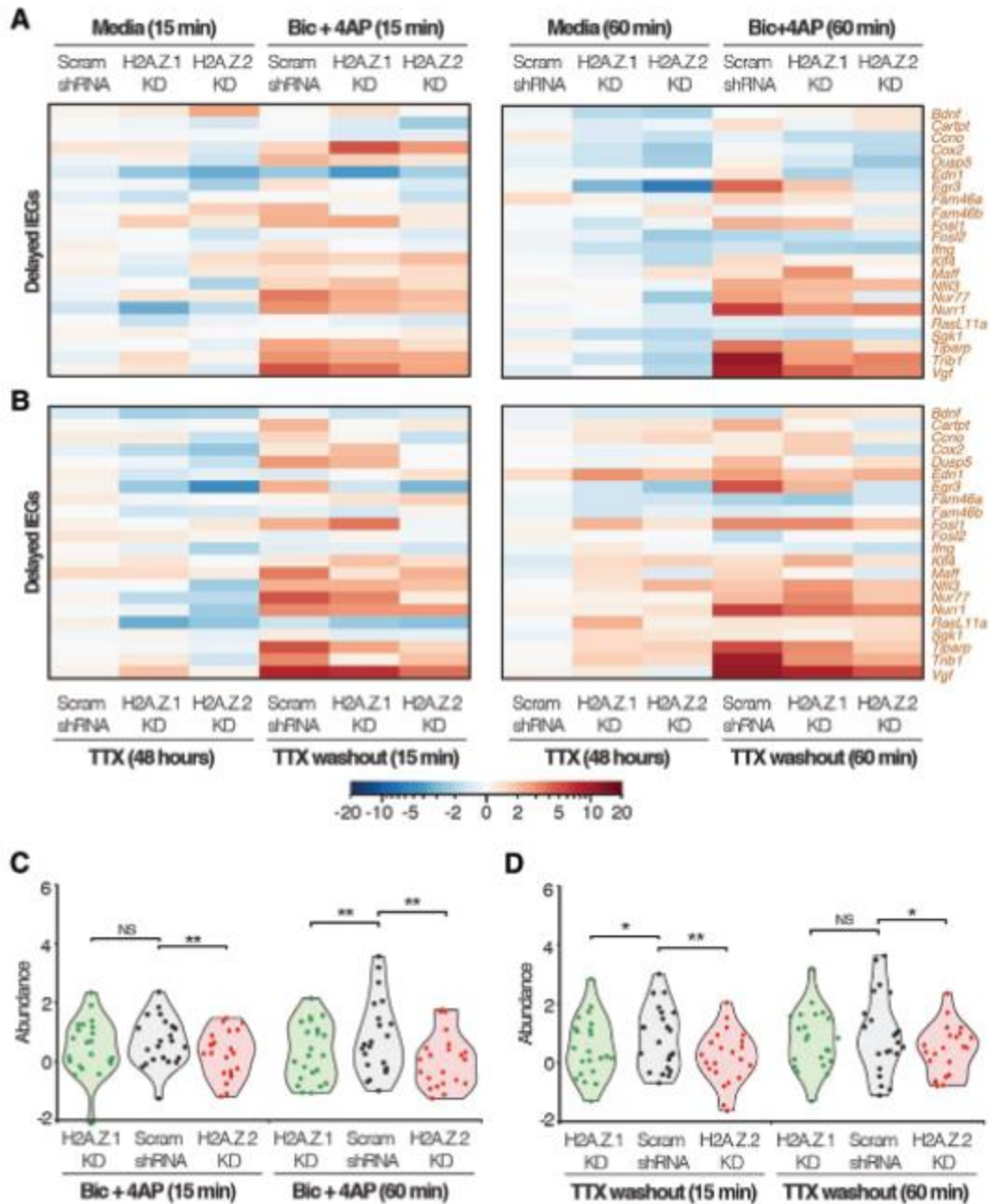


Figure 2-6 Effect of H2A.Z hypervariant depletion on transcription of delayed IEGs. A. Nanostring multiplexed gene expression data (heat maps) representing pre-mRNA levels in control and hypervariant-depleted neurons treated with Bic+4AP for indicated times. B. Heat map representing pre-mRNA levels in control and hypervariant-depleted neurons treated TTX for 48 h followed by washout and collected at indicated times. C, D. Violin plots depicting pre-mRNA abundance of all delayed IEGs from hypervariant-depleted neurons compared to that of control neurons treated with Bic+4AP (C) or TTX for 48 h followed by washout (D) for indicated times. $N = 3$ for each treatment at all time points. * $p < 0.05$ and ** $p < 0.01$ (Wilcoxon paired nonparametric test)

2.3 Discussion

H2A.Z is enriched in nucleosomes near promoters and enhancers of many vertebrate genes and therefore is postulated to play a critical role in gene transcription [Farris et al, 2005; Raisner et al, 2006; Zlatanova et al, 2008]. However, roles of the hypervariants H2A.Z.1 and H2A.Z.2 in these processes have often been presumed to be redundant and have not been categorically questioned [Soboleva et al, 2014]. In the current study, we have demonstrated multiple non-redundant effects of H2A.Z.1 and H2A.Z.2 in transcriptional regulation: (1) H2A.Z.1 and H2A.Z.2 depletion differently influence activity-induced *Arc* transcription kinetics; (2) in resting neurons, H2A.Z.2, but not H2A.Z.1, is required near the *Arc* TSS for RNA Pol II pausing; (3) activity-induced transcription of certain IEGs is sensitive to depletion of only one of the two hypervariants (e.g., *Btg2* and *Dusp1* response is less after H2A.Z.2, but not H2A.Z.1, knockdown); and (4) certain IEGs appear to be differentially sensitive to one or both hypervariants in a context-dependent manner (*Fbxo33* and *Maff* after H2A.Z.1 depletion, *Fam46a* after loss of H2A.Z.2). Taken together, the data presented herein strongly suggest that H2A.Z hypervariants have important, nonredundant roles and/or functional specificity that should be considered for a full understanding of the role of H2A.Z in gene transcription.

Three lines of evidence inspired our hypothesis about functional specificity of H2A.Z hypervariants. First, several instances have been observed in nature where genes duplicated during evolution encode very similar protein products that have achieved functional diversity. Because mechanisms that work are often preserved in nature, we reasoned that the three amino acid differences in these hypervariants might be enough to allow functional diversity. Second, all three variant amino acid residues reside in functionally pertinent regions thereby making them suitable to mediate alternative functionalities.

H2A.Z.1^{14S}/H2A.Z.2^{14A} is located in the H2A.Z N-terminal tail, which is heavily acetylated and is linked to H2A.Z transcriptional activity [Bruce et al, 2005; Valdes-Mora et al, 2012]. H2A.Z.1^{38T}/H2A.Z.2^{38S} is located at the edge of the L1 loop, which plays an essential part in intranucleosomal interactions of H2A.Z [Horikoshi et al, 2013]. Such intranucleosomal interactions are also facilitated by the unstructured region of H2A.Z C-terminus [Wrattling et al, 2012], which houses the H2A.Z.1¹¹²^{128V}/H2A.Z.2^{128A} variation. Third, knockout of H2A.Z.1 results in embryonic lethality in mice [Faast et al, 2001] indicating that H2A.Z.2 cannot compensate for the loss of its paralog. Together, these observations suggest that H2A.Z hypervariants have nonredundant functions that have yet to be adequately explored.

Our study into functional specificity of H2A.Z hypervariants in activity-induced *Arc* transcription revealed a few interesting aspects of H2A.Z biology. Overall, *Arc* transcription requires both H2A.Z.1 and H2A.Z.2. Depletion of either hypervariant had unique effects on *Arc* transcriptional kinetics that were not compensated by the other paralog. In resting neurons (i.e., without homeostatic changes induced

by silencing), H2A.Z.2, but not H2A.Z.1, was found to be necessary for the rapid phase of activity-induced *Arc* transcription (within 15 min of treatment) by facilitating RNA Pol II promoter proximal pausing (Figures 2-3, 2-4). In comparison to the Pol II pausing-related defined role of H2A.Z.2 in *Arc* transcription, the exact role of H2A.Z.1 in the process is less apparent. In normal, un silenced neurons, lack of H2A.Z.1 impairs only the late segment of activity-induced *Arc* transcription (30 min and later). As suggested by our DRB washout assays, this is most likely via indirect mechanisms (discussed further below). However, after subjecting neurons to homeostatic plasticity-related changes with TTX exposure for 48 h, H2A.Z.1 depletion also impairs early responses of *Arc* transcription. This repurposing of H2A.Z.1 after prolonged lack of activity could be mediated by a context-dependent newfound ability to facilitate Pol II pausing. Alternatively, these data could also be explained by heterogeneity of nucleosomal composition in the cell population (discussed further below).

It is possible that these *Arc* TSS nucleosomal loci are populated by different H2A.Z hypervariants in different alleles and/or cells in the population. In resting neurons, only the fraction of these alleles and/or cells that have H2A.Z.2, and therefore paused Pol II, responds to activity. After prolonged TTX treatment, additional alleles and/or cells with H2A.Z.1 could attain Pol II pausing via unknown mechanisms and facilitate an enhanced response after TTX washout. This explanation aligns with the noticeably more robust expression of *Arc* after prolonged TTX treatment and washout in comparison to disinhibition-induced activity under previously untreated conditions (compare Figures 2-3 B and 2-5 B). Also, the effect of H2A.Z.1 depletion on late, not early, *Arc* transcriptional response (Figure 2-3 B) falls within the scope of this explanation. Upon induction of activity in resting conditions, H2A.Z.1-containing alleles and/or cells undertake *Arc* transcription in a Pol II pausing-independent 'delayed' fashion, as delayed IEGs do [Saha et al, 2011], thereby accounting for impairments at later time points in H2A.Z.1-depleted neurons. These are exciting possibilities that will require further probing.

Additional experiments will also be required to understand the relevance of the H2A.Z chaperone ANP32E in regulating H2A.Z functions [Mao et al, 2014; Obri et al, 2014]. The H2A.Z.2 loss phenotype was partially rescued by co-depletion of ANP32E. Because ANP32E removes H2A.Z from nucleosomes [Gursoy-Yuzugullo et al, 2015; Mao et al, 2014; Obri et al, 2014], it is likely that the presence of ANP32E in H2A.Z.2-depleted neurons facilitates continued removal of nucleosomal H2A.Z.2 and subsequent fallouts thereof, including loss of Pol II pausing and inability to respond rapidly. However, co-depletion of the chaperone along with the histone preserves nucleosomal H2A.Z.2, at least in part, enabling *Arc* to rapidly respond to some extent. A similar precedence of H2A.Z and ANP32E co-depletion partially rescuing phenotype loss due to depletion of one of these factors was demonstrated in non-neuronal cells [Alatwi et al, 2015]. Our findings, combined with this previous report, advocate for the need to approach the complex biology of H2A.Z hypervariants and their chaperones together.

Collectively, our current studies indicate that H2A.Z hypervariants mediate activity-induced IEG transcription in a context-dependent (H2A.Z.1) or context-independent (H2A.Z.2) fashion, where the extent of their involvement in the transcriptional process varies from gene to gene. Our data also suggest spatial and temporal cooperation of these hypervariants in manifesting the maximum gene response under a given circumstance. Finally, it is our hope that the data presented here will increase appreciation for functional specificity of H2A.Z hypervariants and promote tool-building efforts to enable a comprehensive understanding of diverse roles played by these paralogs at different genes and under different neurobiological contexts.

2.4 Future Directions

Natural follow-up to this work includes experimenting with point mutations that change H2A.Z.1 into H2A.Z.2 one amino acid at a time, developing a better understanding of the differential roles of H2A.Z hypervariants in transcription after homeostatic changes, and working to elucidate the role of these hypervariants during neurodevelopment.

Table 3. List of point mutations targeted at amino acid differences between H2A.Z.1 and H2A.Z.2

Name	Position	Original AA (Z1)	Substituted AA (Z2)
A14T	14	Thymidine	Alanine
T38S	38	Serine	Thymidine
A128V	128	Valine	Alanine

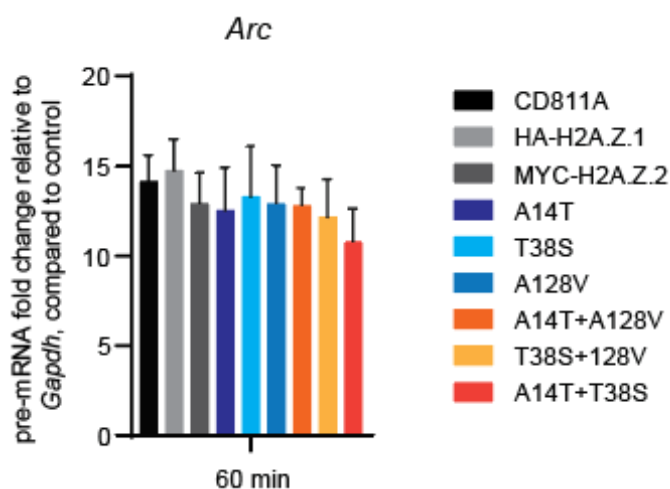


Figure 2-7 Preliminary investigation into amino acid differences between H2A.Z hypervariants. Representation of Arc pre-mRNA levels in neurons expressing exogenous constructs encoding normal H2A.Z.1, normal H2A.Z.2, three single point mutants, and three double mutants. Mature neurons were infected for 5 days and gene expression was induced by treating cells with Bic+4AP for 60 min; data expressed as fold change relative to *Gapdh* and compared to CD811A empty-vector control. $N = 3$.

Preliminary investigation into whether one or more of the amino acid differences between H2A.Z.1 and H2A.Z.2 play a larger role in observed phenotypes is shown in Figure 2-7. Separate lentiviral vectors driving exogenous expression of H2A.Z.1, H2A.Z.2, each of the three single mutants (see Table 1), and the three potential double mutants were developed in the lab. Mature neurons were infected with one of nine viruses (8 H2A.Z-type plus CD811A control) for 5 days, and then neuronal activity was induced using the Bic+4AP protocol. We observed no significant difference in activity-induced expression of *Arc* pre-mRNA across all samples (Figure 2-7). This is most-likely due to the presence of endogenous H2A.Z proteins. As mentioned previously, we found that infecting with multiple viruses increased the viral load enough to cause cell death, which prevented us from being able to deplete neurons of endogenous H2A.Z proteins while also expressing exogenous constructs. Although we did verify nucleosomal incorporation of HA- and MYC-tagged constructs [Dunn et al, 2017], it will be important for future studies to verify that exogenously expressed point mutants are also incorporated into nucleosomes. Future attempts at approaching this question would benefit from combining exogenous expression of mutants with depletion of the endogenous pool of H2A.Z proteins, and tool-building efforts will be necessary to achieve this.

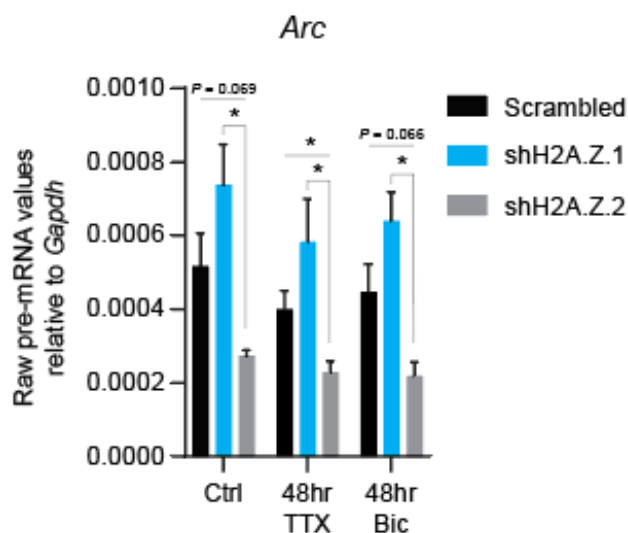


Figure 2-8 Differential regulation of *Arc* expression in homeostatically challenged neurons after H2A.Z hypervariant depletion. Representation of *Arc* pre-mRNA expression in neurons treated with either TTX or Bic for 48hr followed by washout; samples collected 15 min after washout. Data represented as raw pre-mRNA values relative to *Gapdh*; $N = 3$; * represents $p < 0.05$

We observed differential effects on regulation of rapid IEG transcription in cells depleted of either H2A.Z hypervariant when forced to undergo homeostatic changes [Dunn et al, 2017]. The homeostatic challenge in that study utilized TTX, which prevents synaptic activity by blocking voltage-gated sodium channels.

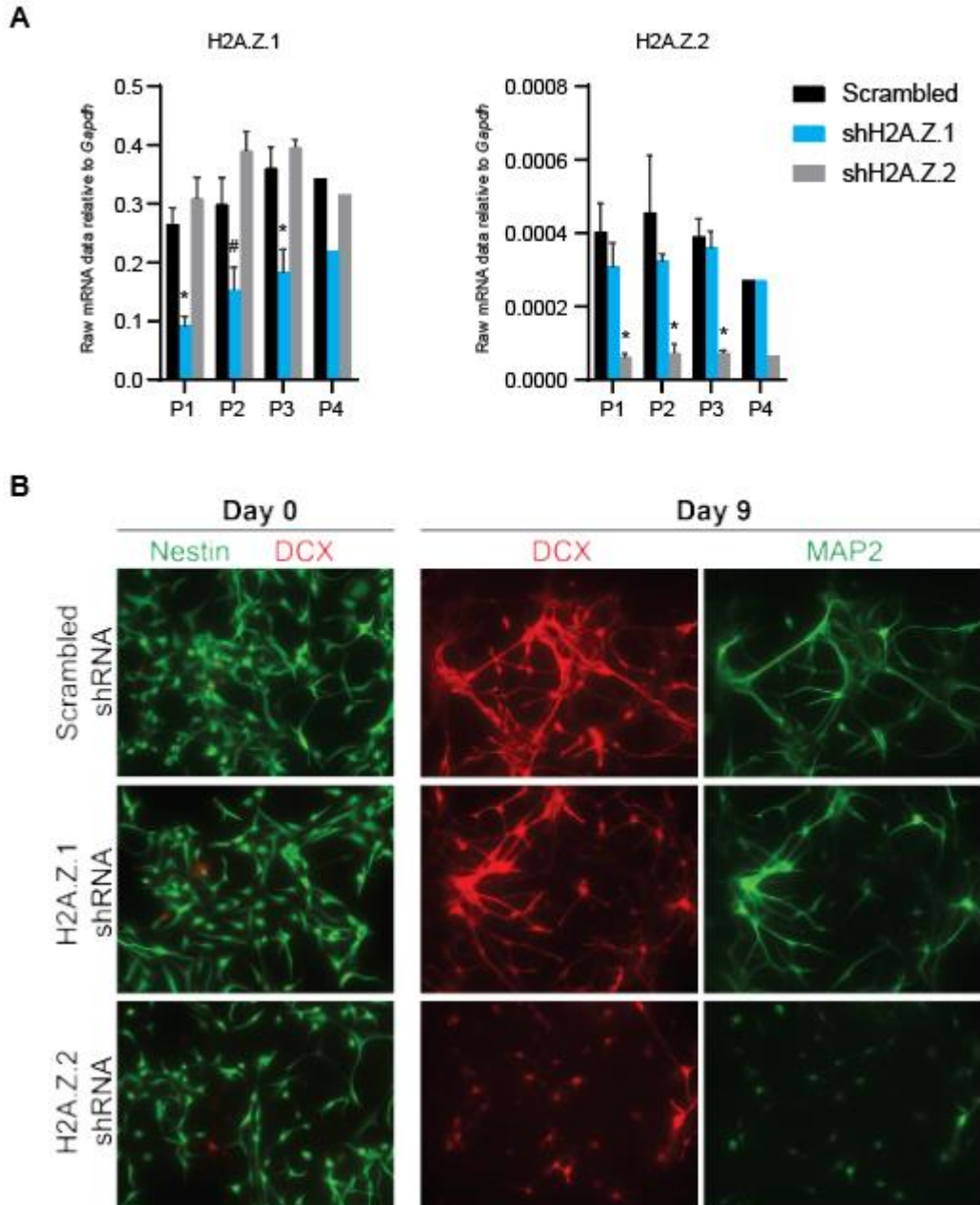


Figure 2-9 Effect of H2A.Z depletion on neuronal development. A. shRNA-mediated knockdown of H2A.Z.1 (left) and H2A.Z.2 (right) in neuronal progenitor cells over the course of 4 passages; raw data represented relative to *Gapdh*; $N = 3$ for P1-P3 and $N = 1$ for P4; * represents $p < 0.05$, # represents $p = 0.064$ B. Representative ICC images showing expression of Nestin and DCX in NPCs (Day 0), and DCX and MAP2 in developing neurons (Day 9) depleted of either H2A.Z.1 or H2A.Z.2 before the onset of differentiation; notation at top represents time after the onset of differentiation

However, neurons adjust to maintain homeostasis when there is minimal activity (simulated by prolonged TTX treatment) and when there is too much activity. We simulated an overactive environment by treating mature neurons with Bic (50 μ M) for 48hr and compared washout-induced expression of Arc in those cells to that in control cells and cells treated with TTX for 48hrs (Figure 2-8). In both types of homeostatic challenge, loss of H2A.Z.1 seems to cause an increase in Arc expression, while loss of H2A.Z.2 results in decreased transcription. Further investigation into the dynamics of hypervariant incorporation into nucleosomes near promoters as neurons are adjusting to maintain homeostasis will be required to fully understand the mechanisms by which each hypervariant is involved in regulating rapid IEG transcription in different cellular environments.

Early efforts to study the role of H2A.Z in mammalian development discovered that loss of H2A.Z.1 is embryonic lethal [Faast et al, 2001]. Development of more advanced genetic engineering tools has recently allowed scientists to study the effects of brain-specific H2A.Z knockout on neurodevelopment [Shen et al, 2018]. However, given the evidence presented strongly supporting non-redundant functions of H2A.Z hypervariants in regulation of gene transcription, making an effort to elucidate the differential roles of H2A.Z.1 and H2A.Z.2 during neurodevelopment will be imperative to our understanding of the overall process.

We were able to successfully knockdown each hypervariant in neural progenitor cells (NPCs) with the same lentiviral constructs used in our previous study [Dunn et al, 2017]. We tracked knockdown in dividing progenitors over the course of four passages and observed consistent knockdown of H2A.Z.2. Knockdown in NPCs infected with shH2A.Z.1, however, seemed to be less efficient over time (Figure 2-9 A). We postulated that, since lentiviral infections are rarely 100% efficient and we know from previous studies that loss of H2A.Z.1 is embryonic lethal [Faast et al, 2001], some cells infected with higher titers of shH2A.Z.1 could be dying and those that were not infected in the population would continue to divide decreasing the overall knockdown efficiency in the population over time. With that idea in mind, our subsequent experiments investigating the roles of H2A.Z hypervariants in neuronal differentiation were conducted using NPCs that were only passaged once.

The process of neurodevelopment has multiple stages, including proliferation, differentiation, migration, and maturation. We started out by conducting preliminary experiments to better understand the involvement of H2A.Z.1 and H2A.Z.2 in the differentiation of neural progenitor cells to neurons. We used an established protocol to differentiate NPCs (derived from E14 rat cortices) to neurons (see Methods). We performed ICC on NPC samples before the onset of differentiation and probed for Nestin (NPC marker) and Doublecortin (DCX; immature neuron marker) to assess the developmental status of our cellular

population. It appears at though loss of H2A.Z hypervariants does not cause premature differentiation (Figure 2-9 B, Day 0). Nine days after the onset of differentiation *in vitro*, we again performed ICC, this time probing for DCX and MAP2 (neuronal dendritic marker). While loss of H2A.Z.1 does appear to affect differentiation (based on expression of these markers), loss of H2A.Z.2 appears to severely decrease arborization of developing neurons (Figure 2-9 B, Day 9).

Based on the results of our differentiation experiment, we sought to understand the mechanism by which loss of H2A.Z.2 could be negatively affecting, or even preventing, neuronal differentiation. At a foundational level, changes in cellular state require the simultaneous coordination of expression and repression of different cohorts of genes. This molecular harmony is achieved, in large, by chromatin remodeling complexes that function to make different parts of the genome accessible, or unavailable, to transcription machinery depending on the needs of the cell. One family of chromatin remodelers that is heavily involved in neurodevelopment is the Brg1/BRM associated factor (BAF) complex family. It has been demonstrated that the subunit composition of BAF complexes changes with cellular state. For example, embryonic stem cell BAF (esBAF) complexes have a slightly different subunit composition that neural progenitor BAF (npBAF) complexes, and npBAF also differs from neuronal BAF (nBAF) in subunit composition [Bachmann et al, 2016; Lessard et al, 2007; Wu et al, 2007]. We hypothesized that H2A.Z hypervariants could be differentially involved in regulating transcription of genes encoding BAF complex subunits during neuronal development. To investigate this possibility, we first analyzed the effects of hypervariant loss on expression of nBAF complex subunit mRNA in mature neurons (Figure 2-10 A). We found expression of 12/19 genes to be significantly affected by hypervariant loss. Interestingly, about half of the genes affected by hypervariant loss showed similar phenotypes for both hypervariants, and only two of the genes affected showed a decrease in expression.

Next, we asked how loss of hypervariants in NPCs effects expression of genes encoding both npBAF and nBAF subunits (Figure 2-10 B). Unexpectedly, we found no significant difference in expression of any genes due to hypervariant loss. Future experiments should include an assessment of gene expression at different time-points throughout differentiation in cells depleted of either hypervariant. It may be true that hypervariant loss alters the temporal progression of differentiation (Figure 2-11), so this approach might lend more insight, given the H2A.Z.2 phenotype observed in Figure 2-9). It's important to note that increased mRNA expression does not necessarily lead to increased protein expression, and increased protein expression does not dictate functional incorporation into a complex. Further experimentation is required to fully understand the role of H2A.Z hypervariants in the regulation of BAF complex subunit composition and/or function during different stages of neurodevelopment.

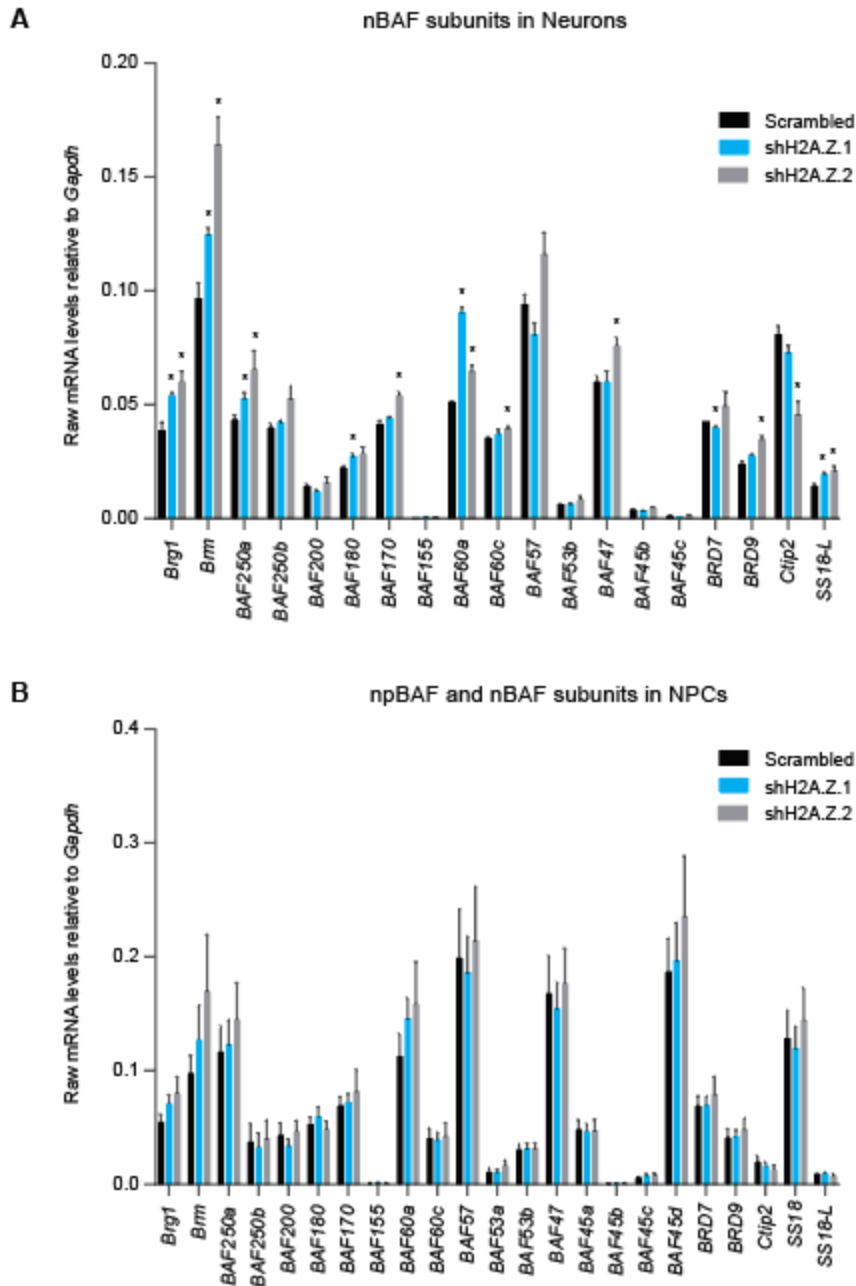


Figure 2-10 Effects of H2A.Z hypervariant loss on expression of BAF complex subunits in neurons and NPCs. A. Representation of mRNA levels of neuron-specific BAF (nBAF) complex subunits in mature neurons depleted of either H2A.Z.1 or H2A.Z.2; data represented as raw mRNA values relative to *Gapdh*; $N = 3$; * represents $p < 0.05$. B. Representation of mRNA levels of NPC-specific BAF (npBAF) and nBAF complex subunits in NPCs depleted of either H2A.Z.1 or H2A.Z.2; data represented as raw mRNA values relative to *Gapdh*; $N = 4$

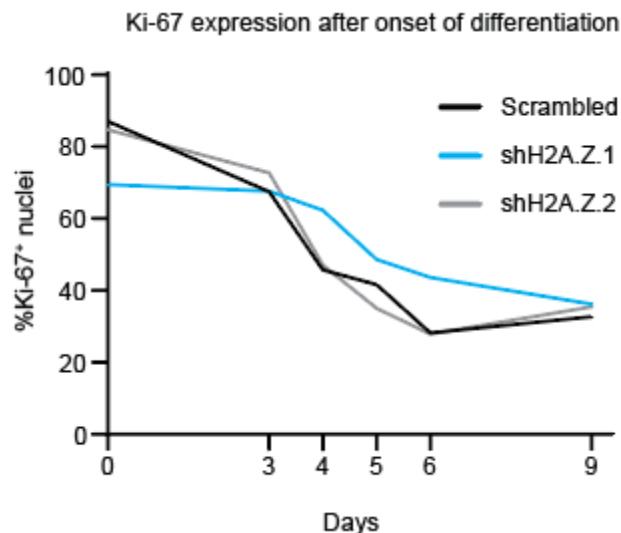


Figure 2-11 Preliminary investigation into effects of hypervariant loss on neuronal differentiation. Quantification of fluorescent images taken of differentiating neurons probed with an antibody against Ki-67 and stained with DAPI. 1,000+ cells were counted for each knockdown condition at each time-point after the onset of differentiation. Representative images were counted by four different people, and the average %Ki-67 positive nuclei were plotted here. $N = 1$ for each time-point.

Our initial knockdown trials (Figure 2-9 A) suggested that hypervariant loss may differentially affect cell cycle dynamics in proliferating NPCs, so we designed some experiments to preliminarily continue this line of questioning. First, we conducted a proliferation assay utilizing a nucleoside analog (EdU) that can be labeled and detected by fluorescence. Hypervariant-depleted NPCs were pulsed with EdU for 1hr and ICC was subsequently performed to label the nucleoside analog and total DNA (using DAPI). Random images were taken of each sample using the Keyence BZ-9000 Fluorescent Microscope, and an automated pipeline in ImageJ was used to detect DAPI⁺ nuclei and measure relative EdU fluorescence. Using a nonparametric statistical analysis (Mann-Whitney), we found that loss of either hypervariant results in less EdU incorporation (Figure 2-12), which suggests that H2A.Z hypervariants are involved in regulating cell cycle dynamics to some extent.

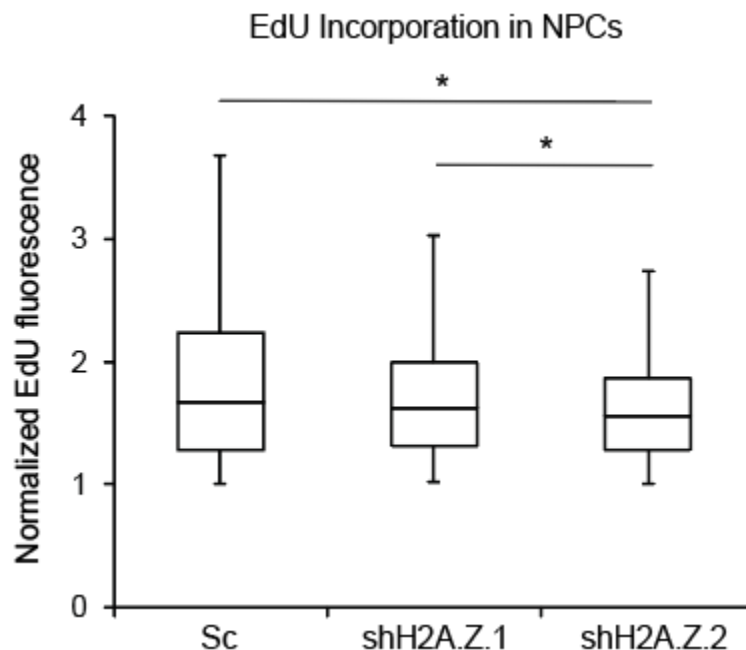


Figure 2-12 Preliminary investigation into effects of hypervariant loss on NPC proliferation. Quantification of EdU incorporation into dividing neuronal progenitors treated with the nucleoside analog for 1 hr. 1000+ cells were counted for each knockdown condition automatically in ImageJ. Relative fluorescence was measured in DAPI positive cells and normalized to background fluorescence of each individual image. Threshold for normalized EdU detection was set at 1. $N = 3$; * represents $p < 0.001$; Mann-Whitney test

Next, we analyzed cell cycle dynamics in hypervariant-depleted NPCs by staining cells with propidium iodide (PI; fluorescent DNA-binding agent) and performing flow cytometry. Figure 2-13 B shows representative flow plots from our experiments. It appears as though loss of H2A.Z.1 results in more apoptotic cells (note population of sample within red box). The results of two biological replicates was quantified in Figure 2-13 C. Note the decrease in shH2A.Z.1-treated cells at G1/G0 seems to be mirrored by the increase in apoptotic shH2A.Z.1-treated cells. This preliminary analysis suggests that the apoptotic fraction of cells depleted of H2A.Z.1 may not be able to enter the G1/G0 phase. Follow-up investigations should include an analysis of the effects of hypervariant loss on expression of genes encoding cell cycle regulators in NPCs.

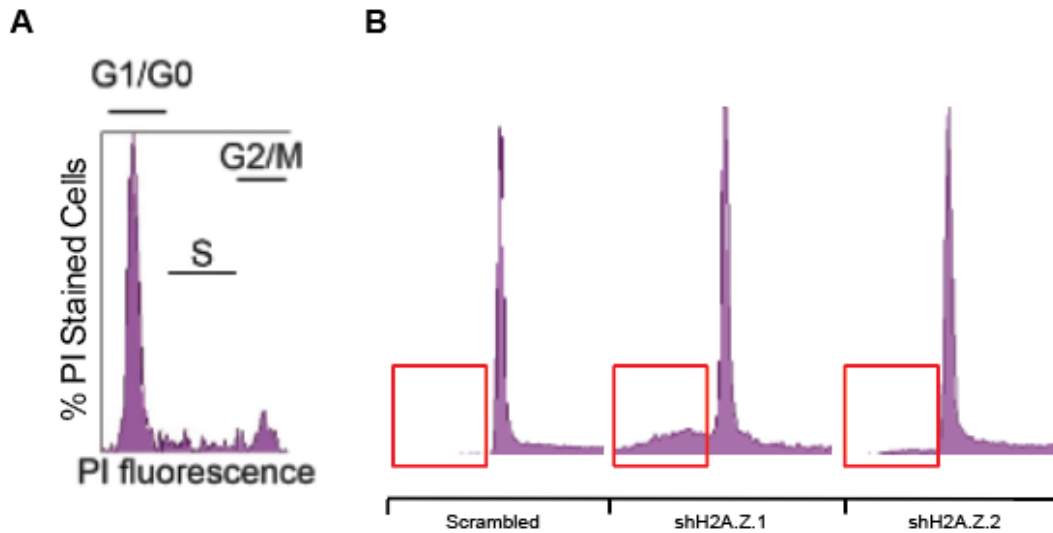


Figure 2-13 Preliminary investigation into effects of H2A.Z hypervariant loss on cell cycle dynamics in NPCs. A. Example of annotated results of flow cytometry analysis using propidium iodide (PI). B. Representative flow plots from 1 of 2 biological replicates performed in NPCs depleted of either H2A.Z hypervariant and treated with PI. Red boxes highlight apoptotic fraction of each sample; $N = 2$. C. Quantification of PI-stained cells in each phase of the cell cycle and those undergoing apoptosis; $N = 2$

Our understanding of the differential roles of H2A.Z hypervariants in brain function is in its early stages. As our collective ability to develop genetic and molecular tools continues to advance, it will become more feasible to map the epigenomic landscape in neural cell types at different stages of development and we must take histone variants into account as we do so to fully understand the mechanisms of transcriptional regulation in the brain.

2.5 Materials and Methods

2.5.1 Isolation and culture of primary rat neurons

All experiments were carried out according to University of California (UCM) and National Institute for Environmental Health Sciences (NIEHS) Institutional Animal Care and Use Committee (IACUC) regulations. Cortical neurons were isolated from embryonic day 18 (E18) Sprague Dawley rats, and single cell suspensions

were prepared by triturating minced cortices through a fire-polished Pasteur pipet using either Hank's Balanced Salt Solution without Calcium and Magnesium (Invitrogen) or Accutase (Invitrogen). Dissociated neurons were plated in Neurobasal medium (Invitrogen) supplemented with 0.5mM GlutaMAX-I (Invitrogen), 25 μ M glutamate (Sigma-Aldrich), and either B27 (Invitrogen) or NS21. Cells were maintained up to 14 days in a similar medium without glutamate. NS21 was prepared as previously described [Chen et al, 2008]. Cells were used for gene induction experiments between 10-14 days *in vitro* (DIV), at which time synapses have formed and are functional.

2.5.2 *Infection with recombinant viruses*

Viral supernatant was diluted in culture media at dilutions between 1:50 and 1:10. Cells were routinely infected between 5-7 DIV, and experiments were performed 4-7 days after infection.

2.5.3 *Inducing gene expression in vitro*

To utilize synaptic activity to induce gene expression, resting cortical neurons were co-treated with Bicuculline (Bic; 50 μ M; Sigma-Aldrich) and 4-aminopyridine (4AP; 75 μ M; Acros Organics) [Papadia et al, 2005]. To induce gene transcription intracellularly (by-passing the synapse), neuronal activity was blocked by treating the cells with Tetrodotoxin (TTX; 1-2 μ M; Calbiochem) and the MAPK pathway was activated with phorbol ester myristate (PMA; 1 μ M; Sigma-Aldrich). To induce transcription

intranuclearly, neurons were treated with 5, 6-dichloro-1- β -D-ribofuranosylbenzimidazole (DRB; 100 μ M; Sigma-Aldrich) alone or co-treated with Triptolide (Trip; 250-500nM; Tocris) for 1 hour followed by washout with pre-conditioned media. To induced gene expression after a homeostatic change, neurons were treated with 1-2 μ M TTX for 48 hours followed by a series of washouts with pre-conditioned media as described previously [Saha et al, 2011].

2.5.4 *Isolation of RNA and quantification of gene expression*

Total RNA was isolated from dissociated cortical neurons using the RNeasy Mini Kit (QIAGEN) and DNA was removed from the sample using an in-column DNase digestion kit (QIAGEN). cDNA synthesis and subsequent amplification of pre-mRNA was achieved using primers specifically designed to target the intron-exon borders of desired genes [Saha et al, 2011] and the One-Step RT-PCR kit (QIAGEN). cDNA synthesis and subsequent amplification of mRNA was achieved using MuLV reverse transcriptase (Promega), random hexamers and oligo dT primers (Promega), and RNase inhibitors (Thermo Scientific). Quantification of gene expression was achieved by performing quantitative RT-

PCR (qRT-PCR) using iTaq Universal Sybr Green Supermix (BioRad) and the BioRad CFX Connect real-time PCR Detection System.

2.5.5 *Western blotting and detection*

Protein samples were isolated in RIPA buffer, denatured in Laemeli Buffer (BioRad) + β -mercaptoethanol on a heat block at 95°C for 5 min, and resolved on 4-20%, 4-15%, or 8-16% Mini-PROTEAN gels (BioRad) in 1X Tris/Glycine/SDS (BioRad) buffer. The BioRad TBT RTA kit and protocol were used to transfer resolved proteins onto LV PVDF membranes (BioRad). Membranes were incubated at 4°C overnight with primary antibodies in 1X TBS-T (Invitrogen) with 0.5% bovine serum albumin (BSA; Fisher Scientific), washed thrice with 1X TBS-T, incubated on a rocker with appropriate secondary antibody at room temperature for 30-60 minutes, washed thrice with 1X TBS-T, and imaged using the BioRad ChemiDoc Imaging System.

2.5.6 *NanoString analysis*

NanoString probes were designed for indicated pre-mRNAs by NanoString technologies and assays were performed following the manufacturer's protocol. Data were processed in R (version 3.3.2), using the limma package (version 3.30.8) from Bioconductor (version 3.4). Data were log₂ transformed, then batch-adjusted within each experiment and time point to account for sample processing errors. The pre-mRNA measurements were normalized using pre-mRNA housekeeper genes. Sample quality and processing were reviewed and confirmed using MA-plots and heat maps at each step. Pairwise comparisons were performed using the limma-voom methodology as previously described. Statistical hits were defined by requiring one sample group mean log₂ signal at least 2, absolute fold change above 1.5, and Benjamini Hochberg adjusted $p < 0.01$. Heat maps were generated using group mean log₂ normalized abundances, centered to the indicated control group mean. Violin plots were generated using the same values, centered to the treated scrambled for the respective group of treatments. Gene class changes per experiment and time point were tested using group mean values in a nonparametric, paired Wilcoxon test, with gene as the pairing factor, to test for coordinated gene changes between treated shH2A.Z.1 or treated shH2A.Z.2 and the corresponding treated scrambled of the same experiment time point [Dunn et al, 2017].

2.5.7 *Isolation and culture of primary rat neural progenitor cells*

All experiments were carried out according to UCM IACUC regulations. Cortices were isolated from E14 Sprague Dawley rats, and single cell suspensions were prepared by incubating cortices in Accutase (Invitrogen) followed by trituration through a fire-polished Pasteur pipet. Dissociated cells were plated on cell culture dishes coated with CELLStart (Invitrogen) in StemPro NSC SFM

complete medium (Knockout DMEM/F12 (Invitrogen), epidermal growth factor (EGF; 20ng/mL; Invitrogen), fibroblast growth factor (FGF; 20ng/mL; Invitrogen), GlutaMAX (2mM; Invitrogen), StemPro Serum-Free Supplement (2%; Invitrogen)). Progenitors were passaged every 2-3 days and experiments were routinely performed between passages 1-4.

2.5.8 *In vitro* differentiation of progenitors to neurons

Dissociated progenitors isolated from E14 rat cortices were plated on CELLStart coated dishes in StemPro NSC SFM complete medium. Cells were passaged onto poly-L-lysine (2 μ g/mL; Sigma-Aldrich) and Laminin (10 μ g/mL; Invitrogen) coated dishes 2 days post-plating, and complete StemPro medium was replaced with complete Differentiation medium (Neurobasal, 2% B-27, 2mM GlutaMAX) 2 days after passaging. After 3 days in Differentiation medium, cells were fed with Differentiation Feeding media (complete Differentiation media supplemented with dibutyryl cAMP (0.5mM; Sigma-Aldrich)). Cells were subsequently fed every 2-3 days and maintained for up to 28 days post-differentiation.

2.5.9 *Immunocytochemistry*

NPCs were plated on glass chamber slides and either maintained as NPCs or differentiated into neurons as described above. Cells were fixed in a bath of 4% paraformaldehyde (PFA; Sigma-Aldrich) in 1X PBS for 15 minutes at room temperature followed by three washes with 1X PBS. Cells were permeabilized with 0.5% Triton X-100 (TX-100; Thermo Fisher Scientific) for 20 minutes at room temperature followed by three PBS washes. Non-specific binding was blocked by incubating samples Blocking Buffer (1X PBS + 10% Goat Serum (Invitrogen)) for 30 minutes at room temperature. Samples were incubated in appropriate primary antibody solution (3% Goat Serum in PBS with appropriate primary antibody at concentrations from 1:50-1:500) at 4°C overnight. The next day, primary antibody solution was aspirated from wells and samples were washed thrice with 0.5% PBS-T. Samples were incubated with appropriate secondary antibody solution (3% Goat Serum in PBS with secondary antibody at 1:2,000) for 45 minutes at room temperature away from light. Following secondary staining, samples were washed twice with 0.5% PBS-T, and once more with 1X PBS before coverslips were mounted using Prolong Anti-fade GOLD (Invitrogen). Mounted slides were left in the dark at room temperature for 24 hours before being imaged with the Keyence BZ-9000 Fluorescent Microscope.

2.5.10 *Statistical analysis*

Biological replicates for each figure are indicated as *N* in corresponding figure legends. Error bars represent standard error of mean throughout this article. Statistical comparison of datasets was performed with the two-tailed Student's *t*

test (with Bonferroni corrections for multiple comparisons), two-way ANOVA, or Wilcoxon paired nonparametric test, unless otherwise stated in the figure legend.

Chapter 3: Investigating How Activity-Induced Signaling Cascades Play Differential Roles in Regulating Neuronal Immediate-early Gene Transcription

3.1 Introduction

Neuronal activity results in increased concentrations of intracellular calcium. Calcium can enter the cell via voltage-gated calcium channels or ligand-gated ion channels [Berridge, 1998; Jonas et al, 1995], and resulting gene induction patterns vary depending on the mode of entry [Bading, 1993; Ghosh et al, 1994; Ginty et al, 1997; Westenbroek et al, 1992]. Well-known calcium-dependent transcription regulators include CaMKs, the serine/threonine protein phosphatase CaN, and MAPKs. The activation of these proteins by intracellular calcium triggers signaling cascades that convey patterns of membrane depolarization to the nucleus, resulting in gene transcription.

A recent study reported that the MAPK pathway is required for recruitment of Pol II to rapid IEG promoters, but that most rapid IEGs were still partially induced in the presence of MAPK inhibitors [Tyssowski et al, 2018]. This suggests that there may be more calcium-dependent signaling cascades involved in regulating expression of rapid IEGs. Of particular interest as a candidate pathway is CaN signaling, especially due to the fact that *Ppp3cc* (gene encoding the catalytic subunit of calcineurin) and many downstream targets of CaN have been reported as schizophrenia candidate genes [Gallo et al, 2018; Marballi et al, 2018].

CaN signaling has been implicated in transcriptional regulation via cytoplasmic dephosphorylation of its known targets (CRTC1, NFATs, MEFs), resulting in their nuclear translocation and subsequent transcriptional regulation [Chin et al, 1998; Flavell et al, 2005; Graef et al, 1999; Greer and Greenberg, 2008; Mao and Wiedmann, 1999; Zhang et al, 2007]. However, whether or not CaN signaling is an indispensable component of rapid IEG transcription remains untested.

3.2 Results

3.2.1 *Inhibition of translation dysregulates activity-induced expression of Arc, but not via MAPK signaling.*

Most rapid IEGs have a conserved gene expression profile, where pre-mRNA levels start to increase quickly upon induction, peak between 10-45 min (depending on the gene), and decrease thereafter, even in the presence of continuous stimulation. Our initial interest in studying superinduction, the observed phenomena of increased gene expression resulting from inhibition of protein synthesis [Cochran et al, 1983; Lau et al, 1987], came from the idea that the molecular mechanism responsible for the consistent downregulation of rapid

IEG expression at later time-points must somehow be blocked by inhibition of *de novo* protein synthesis.

Using *Arc* as a model gene, we first verified the superinduction phenotype using two different inhibitors of protein synthesis, cycloheximide (CHX) and anisomycin (Aniso). We induced gene expression using the Bic+4AP protocol and observed the effects of each inhibitor at different time-points out to three hours (Figure 3-1 A). As expected, increased *Arc* pre-mRNA expression was observed in the presence of both inhibitors, but only after the 30 min time-point. We hypothesized that the mechanisms driving transcription of *Arc* may also be 'superinduced', or that protein synthesis may be necessary to activate a naturally-occurring 'turn-off' signal. To test the former, we induced gene expression by specifically activating the MAPK pathway, a well-known regulator of rapid IEG transcription [Saha et al, 2011; Tyssowski et al, 2018] using a previously established TTX+PMA protocol. We observed that gene expression induced by MAPK pathway activation alone is not affected by inhibition of translation (Figure 3-1 C). This observation is supported by data presented in Figure 3-1 D, showing no effect on pERK expression upon treatment with CHX.

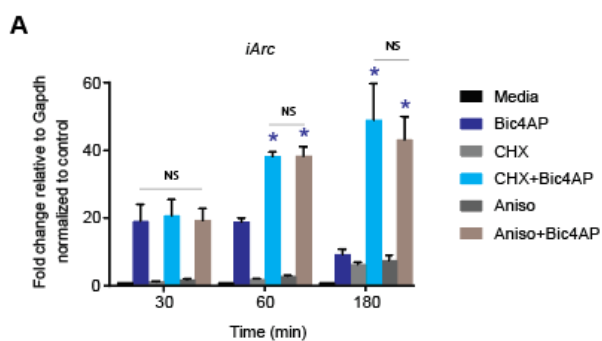
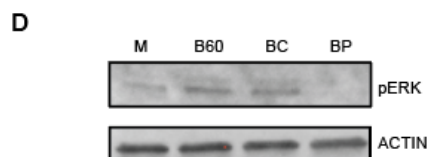
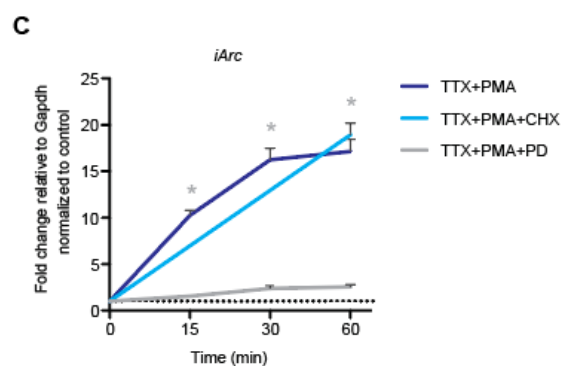
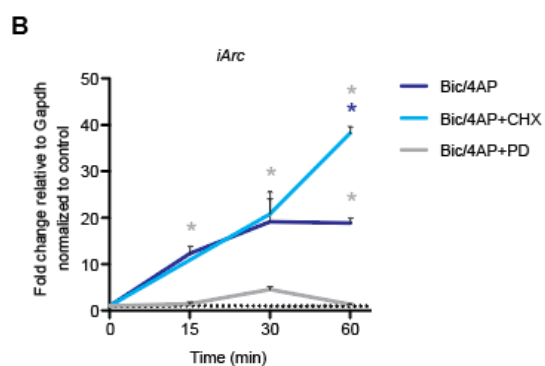


Figure 3-1 Inhibition of translation dysregulates activity-induced expression of *Arc*, but not via the MAPK pathway. A. Representation of *Arc* pre-mRNA expression induced by Bic4AP in the presence or absence of translation inhibitors CHX and Anisomycin at different time-points. Expression shown as fold change relative to *Gapdh*. $N = 5$. B, C. Representation of *Arc* pre-mRNA expression induced by Bic4AP (B) or TTX+PMA (C) in the presence of CHX or PD at different time-points. Expression shown as fold change relative to *Gapdh*. D. Western blot showing pERK expression after 60 min treatments with either Bic4AP (D) in the presence of CHX or PD. Error bars represent SEM; * represents $p < 0.05$



3.2.2 MAPK pathway activation is necessary, but not sufficient to induce optimal transcription of rapid IEGs.

The idea that other signaling pathways may be involved in regulating rapid IEG transcription has been postulated before [Tyssowski et al, 2018], however this hypothesis has yet to be adequately tested. To approach this question, we began

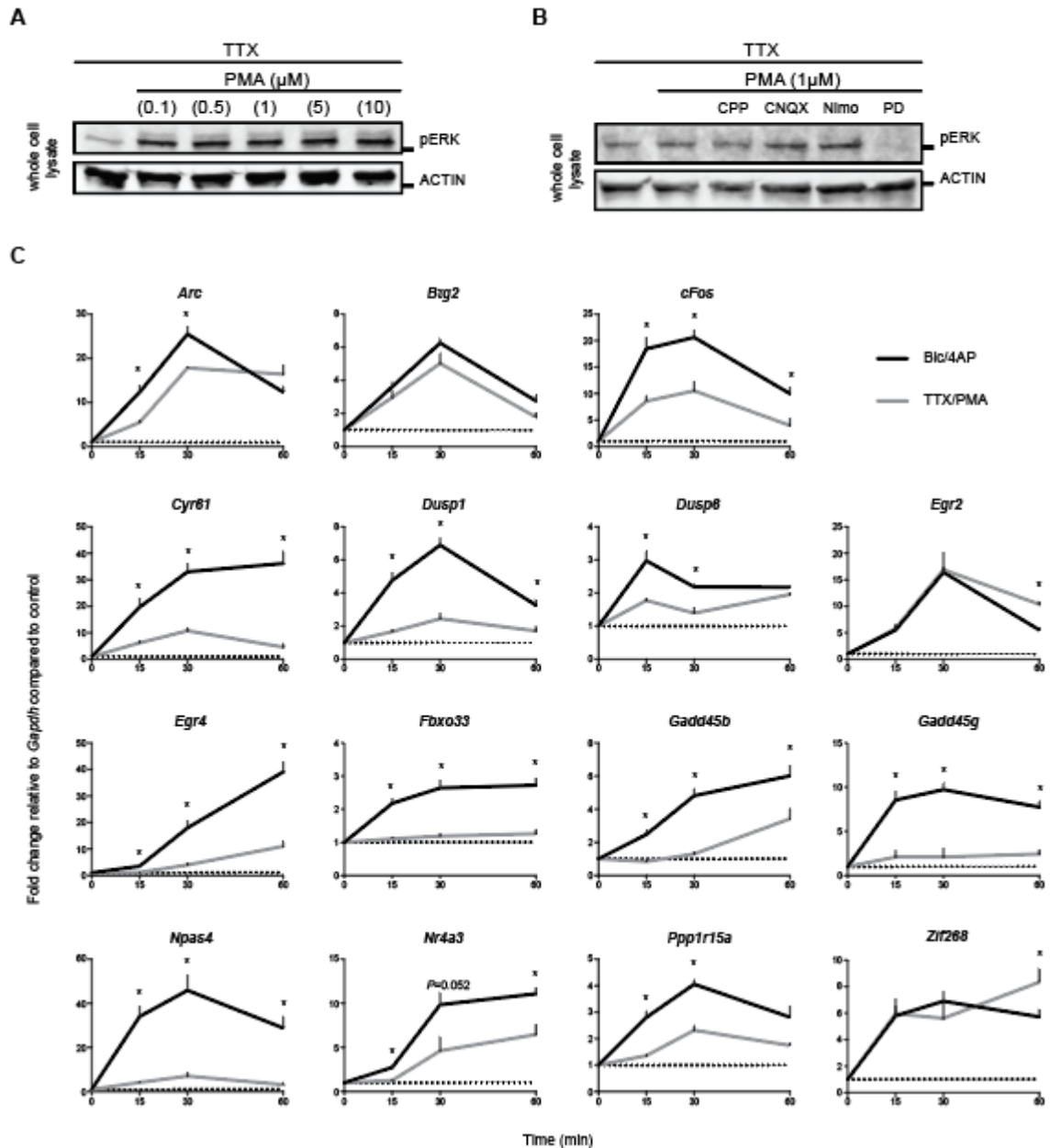


Figure 3-2 MAPK pathway is necessary, but not sufficient to induce optimal expression of rapid IEGs. A. Western blot image showing pERK expression after 30 min treatments with TTX and PMA different concentrations. B. Western blot image showing pERK expression induced by TTX and PMA in the presence of different membrane channel inhibitors and PD. C. Representation of pre-mRNA expression levels of rapid IEGs at multiple time-points in response to treatment with Bic/4AP or TTX/PMA; data expressed as fold change relative to *Gapdh* as measured by qPCR; $N = 3$; * represents $p < 0.05$

by comparing neuronal expression of rapid IEGs induced by either activation of the MAPK pathway alone (TTX+PMA) or by neuronal activity (Bic+4AP). After verifying that our MAPK-specific induction method induced adequate pERK expression (Figure 3-2 A) and does not involve synaptic activation (Figure 3-2 B), we found that MAPK-specific induction fails to optimally induce many rapid IEGs (Figure 3-2 C). If MAPK signaling is not enough on its own, what other signaling pathways are involved in the regulation of rapid IEG expression?

3.2.3 Calcineurin signaling is required for optimal expression of Arc and preventing Calcineurin activation negates the dysregulation of Arc expression induced by inhibition of translation.

Because CaN signaling has been shown to regulate activity-induced transcription [Greer and Greenberg, 2008; Husi et al, 2000; Toliás et al, 2005], we postulated that the phenotype observed upon inhibition of translation could be acting on the Calcineurin pathway. To investigate this, we used a pharmacological inhibitor of CaN activation (FK-506) in combination with CHX and induced gene expression in neurons using the Bic+4AP protocol. We observed that inhibiting CaN activation decreases *Arc* pre-mRNA expression, supporting the idea that CaN signaling is involved in regulating rapid IEG expression. Our results also show that inhibiting CaN activation negates the CHX-induced increase in gene expression, suggesting that the underlying mechanism driving the superinduction phenotype in rapid IEGs involves CaN signaling (Figure 3-3 A). Figure 3-3 A also shows that inhibition of CaN does not significantly affect *Arc* expression at the early time-point. To better understand the dynamics of CaN signaling in regulation of *Arc* expression, we performed a time-course addition of FK-506 in neurons treated with Bic+4AP (Figure 3-3 B) and observed that later addition of the inhibitor does lessen its effect on gene expression at the 30 min time-point (when *Arc* expression is at its peak) but does not differentially affect expression levels at the later time-point.

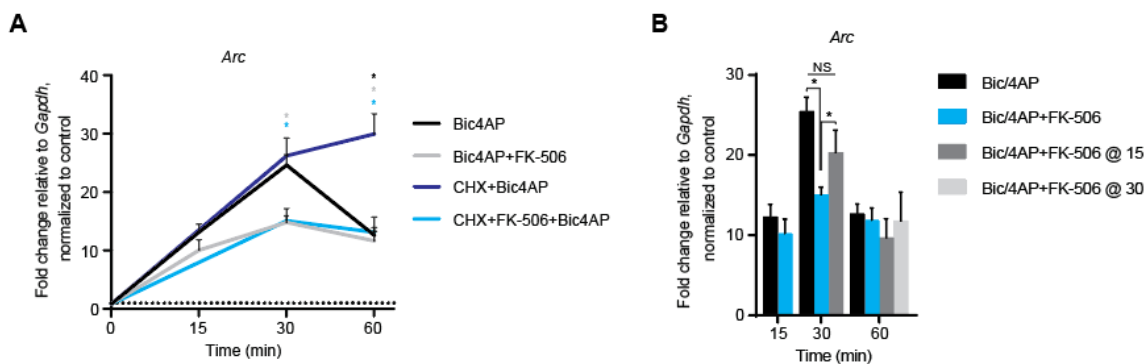


Figure 3-3 Calcineurin signaling is required for optimal expression of *Arc* and preventing Calcineurin activation negates the dysregulation of *Arc* expression induced by inhibition of translation. A. Representation of *Arc* pre-mRNA levels after induction with Bic/4AP in the presence or absence of CHX and FK-506 at different time-points; data expressed as fold change as measured by qPCR; $N = 3-5$. B. Expression of *Arc* pre-mRNA levels after induction with Bic/4AP and addition of FK-506 at indicated time-points during the treatment; data expressed as fold change relative to *Gapdh* as measured by qPCR; $N = 3-5$. * represents $p < 0.05$

3.2.4 Blocking Calcineurin activation does not affect MAPK signaling.

Our evidence thus far supports a combined effort of MAPK and CaN signaling pathways in regulating activity-induced expression of rapid IEGs, but its important to understand whether these pathways are acting on each other or in parallel. To approach this question, we induced the MAPK pathway using PMA (PKC agonist) and Forskolin (PKA agonist) and measured *Arc* pre-mRNA expression in the presence of FK-506, PD, or both (Figure 3-4 A). We verified that pERK expression induced by neuronal activity (Bic+4AP; Figure 3-4 B) or MAPK activation (TTX+PMA+FSK; Figure 3-4 C) is not affected by inhibition of CaN activation. Our data suggests that blocking CaN activation does not affect MAPK pathway function.

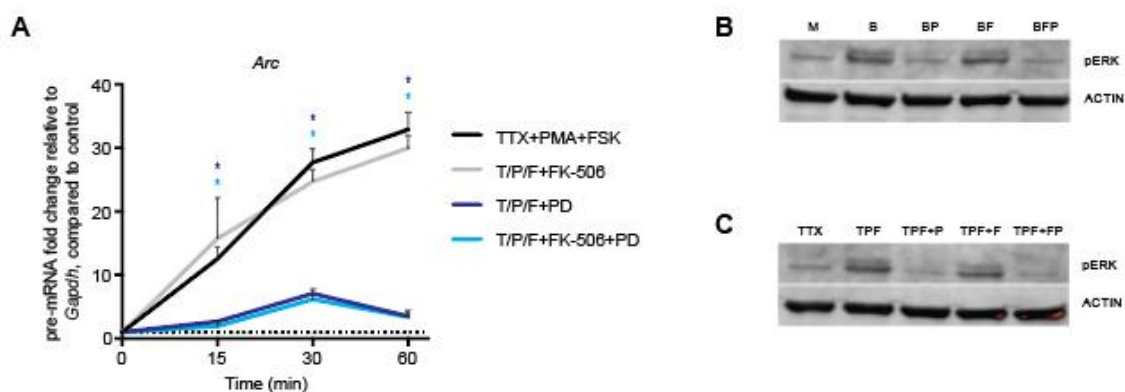


Figure 3-4 Blocking CaN activation does not affect MAPK signaling. A. Representation of *Arc* pre-mRNA in response to treatment with TTX and MAPK pathway activators in the presence of PD, FK-506, or both, at different time-points; data expressed as fold change relative to *Gapdh* as measured by qPCR; $N = 3$; * represents $p < 0.05$. B, C. Western blot from whole cell lysates showing effect of FK-506 and PD (or both) on pERK expression in response to treatment with Bic+4AP (B) or TTX+PMA+FSK (C); $N = 3$

3.2.5 MAPK and CaN signaling pathways are both involved in regulating expression of most rapid IEGs.

The results of our previous experiments suggest that the extent to which MAPK signaling drives expression is not homogenous amongst rapid IEGs (Figure 3-2 C). Therefore, we hypothesized that CaN signaling could differentially regulate expression of rapid IEGs as well. To test this, we induced neuronal activity in neurons using the Bic+4AP protocol and measured pre-mRNA expression of rapid IEGs in the presence of CaN and MAPK pathway inhibitors (Figure 3-5). While most genes in our study were affected by both inhibitors to some extent (and a more severe phenotype was observed upon dual inhibition), these results support the hypothesis that heterogeneity of regulatory mechanisms exists, even in this small cohort of genes. Interestingly, *Egr2* expression actually increased in

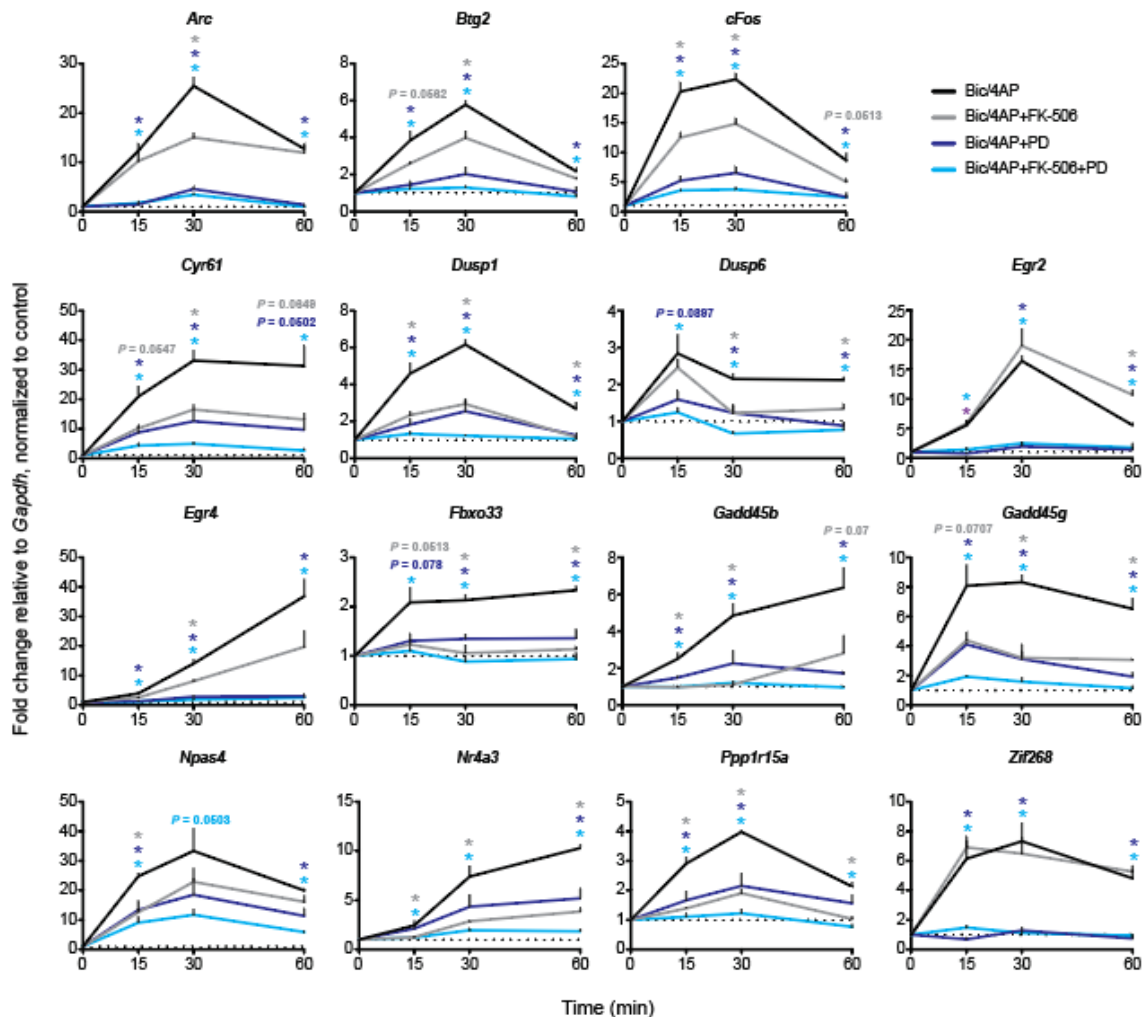


Figure 3-5 CaN and MAPK pathways are both involved in regulating expression of most rapid IEGs. A. Representation of pre-mRNA levels of rapid IEGs after Bic/4AP treatment with CaN and MAPK inhibitors at different time-points; data represented as fold change relative to *Gapdh* as measured by qPCR; $N = 3$; * represents $p < 0.05$

response to treatment with FK-506, and *Zif268* showed no CaN phenotype at any time-point. Of note, inhibition of CaN activation does not significantly affect some of these genes at the early time-point (*Arc*, *Dusp6*, *Egr4*), suggesting that there may be a temporal component to individual pathway involvement in regulation of rapid IEGs.

3.2.6 *Expression of a fraction of rapid IEGs is regulated by Calcineurin – CRTTC1 signaling.*

To better understand the mechanism(s) by which CaN signaling is regulating transcription of rapid IEGs, we decided to investigate the role of CRTTC1 (previously referred to as TORC1), a transcriptional co-activator that has been shown to be incorporated into the nucleus rapidly upon dephosphorylation by CaN [Bittinger, 2004; Greer and Greenberg, 2008], in rapid IEG expression. To ensure that our methods of gene induction involve nuclear incorporation of CRTTC1, we measured its expression in nuclear lysates from neurons treated with Bic+4AP for different lengths of time (Figure 3-6 A). We also generated lentiviruses from a commercially available shRNA construct specific to CRTTC1 and validated knockdown in mature neurons after five days of infection (Figure 3-6 B). We then tested the effect of CRTTC1 knockdown on activity-induced expression of rapid IEGs. Interestingly, not every gene sensitive to CaN inhibition (Figure 3-5) was affected by loss of CRTTC1. This result suggests that CaN signaling may drive expression of individual rapid IEGs via different mechanisms.

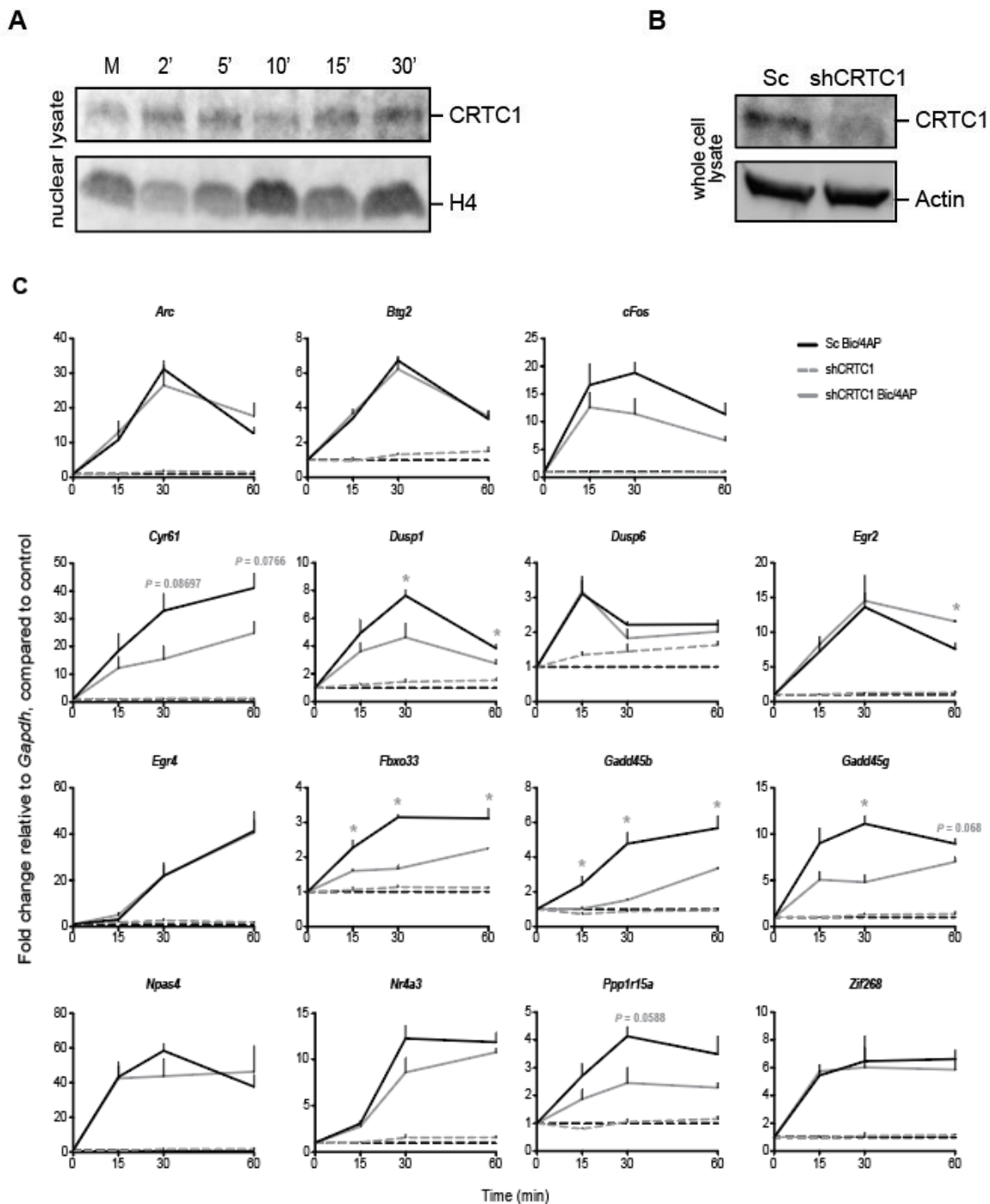


Figure 3-6 Expression of a fraction of rapid IEGs is regulated by Calcineurin - CRTC1 signaling. A. Western blot image showing CRTC1 expression in nuclear extracts of neurons treated with Bic/4AP for indicated times; $N = 2$. B. Western blot image showing CRTC1 expression in neurons infected with a Scrambled shRNA compared to neurons infected with a CRTC1-specific shRNA; $N = 2$. C. Effect of shRNA-mediated loss of CRTC1 on expression of rapid IEG pre-mRNA in neurons treated with Bic/4AP and collected at different time-points; $N = 3$; * represents $p < 0.05$

3.3 Discussion

Immediate-early genes have been broadly split into two categories based on their expression dynamics and what we know about the molecular mechanisms driving their expression [Saha et al, 2011; Tyssowski et al, 2018]. The MAPK pathway has been shown to be indispensable for transcription of rapid IEGs, as it facilitates rapid recruitment of Pol II [Tyssowski et al, 2018]. The work herein illustrates that, while the MAPK pathway is required for optimal expression of rapid IEGs, it is not the only pathway working to drive and regulate activity induced transcription of this class of genes in neurons.

Our investigation into the role of CaN signaling in the regulation of rapid IEG transcription revealed a few interesting insights. Upon blocking activation of CaN, early transcription of some genes, including *Arc*, was not significantly affected (Figure 3-5). We also observed that phenotypic CHX-induced superinduction of *Arc* expression only happens at the late time-point (Figure 3-1 A) and is abolished in the absence of CaN activation (Figure 3-3 A). Together, these findings suggest that CaN signaling may have specific temporal dynamics, and that CaN itself may regulate different downstream effectors that function individually to drive or inhibit transcription.

Throughout this study, the expression dynamics of a few genes stood out under different pharmacological pressures. Specific activation of the MAPK pathway alone was sufficient to optimally induce expression of *Zif268* (Figure 3-2). This gene was also unaffected by FK-506-mediated inhibition of CaN activation (Figure 3-5), suggesting that CaN signaling may not be required for optimal expression of all rapid IEGs. In contrast, *Npas4* was not induced by MAPK pathway activation alone (Figure 3-2) but showed sensitivity to MAPK inhibition (PD treatment) in a different experiment later on (Figure 3-5). It is important to note here that the TTX+PMA method of specific MAPK pathway activation functions via PKC, however PKC and PKA both facilitate activity-induced MAPK function. Further investigation into PKC- versus PKA-specific MAPK activation may lend more insight into the dynamics of MAPK regulation of rapid IEG transcription. There was also a group of genes that were sensitive to CaN inhibition, but not to CRT1 knockdown (*Arc*, *Btg2*, *cFos*, *Dusp6*, *Egr4*, *Npas4*, *Nr4a3*; Figure 3-6). Future studies will be necessary to fully comprehend the complexity with which CaN regulates rapid IEG transcription.

Overall, our observations support the idea that CaN regulates multiple downstream effectors of transcription and may have specific temporal dynamics. These insights highlight the possibility that regulation of rapid IEG transcription is much more complex than previously appreciated.

3.4 Future Directions

A recent report demonstrates that the MAPK pathway is involved in regulating transcription of enhancer RNA (eRNA) [Tyssowski et al, 2018], which is not necessarily surprising given the fact that promoters and enhancers have many genetic features in common [Andersson et al, 2015; Carelli et al, 2018; Carullo et al, 2019; Li et al, 2012; Nguyen et al, 2016; Webster et al, 1988; Zabidi et al, 2015]. Based on this, we wondered if transcription of enhancers can also be superinduced, and if CaN signaling is also involved in regulating eRNA expression. To test this, we observed expression dynamics of the well-characterized enhancer of *Arc*, *SARE* (Figure 3-7). We found that expression of *SARE* 1) can be superinduced (Figure 3-7 A), 2) is sensitive to inhibition of CaN activation (Figure 3-7 B), and 3) exhibits similar temporal dynamics when CaN activation is inhibited at different time-points after induction of neuronal activity

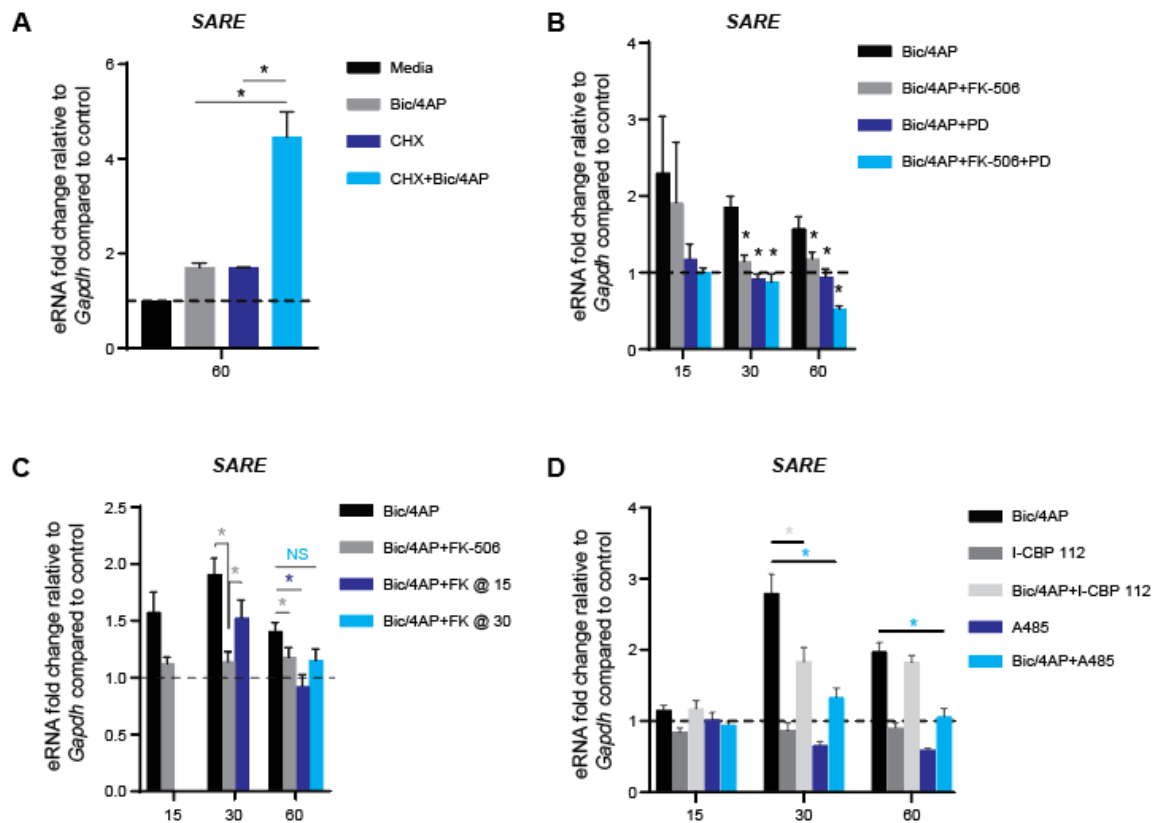


Figure 3-7 Calcineurin signaling and CBP HAT domain regulate expression of *Arc* enhancer, *SARE*. A. Effect of translation inhibition on expression of *SARE* eRNA in neurons treated with Bic/4AP for 60 min. B. Effect of inhibition of Calcineurin activation on expression of *SARE* eRNA in neurons treated with Bic/4AP and collected at indicated time-points. C. Representation of *SARE* eRNA expression in neurons after induction with Bic/4AP and addition of FK-506 at indicated time-points during the treatment. D. Effect of CBP inhibitors on expression of *SARE* eRNA in neurons treated with Bic/4AP and collected at indicated time-points. For all data sets: $N = 3-4$; * represents $p < 0.05$

(Figure 3-7 C). Tyssowski et al. also reported that, while MAPK does regulate eRNA expression, it is not responsible for acetylation of H3K27, a histone post-translational modification that marks active enhancers. It is known that H3K27 is a target of CREB-binding protein (CBP) [Bannister, 1996; Kim et al, 2010; Kwok et al, 1994; Malik et al, 2014; Raisner et al, 2018], and our interest in CBP is also fueled by reports demonstrating that CBP and CRTC1 bind to CREB to regulate transcription [Conkright et al, 2003; Xu et al, 2007]. We have verified that CBP HAT activity is required for optimal activity-induced expression of *SARE* eRNA (Figure 3-7 D), as well as pre-mRNA of many rapid IEGs (Figure 3-8). Of note, our results show that activity-induced expression of both *Npas4* and *Zif268* are not affected by inhibition of CBP HAT activity, which is further evidence of the mechanistic complexity at play regulating expression of this small cohort of

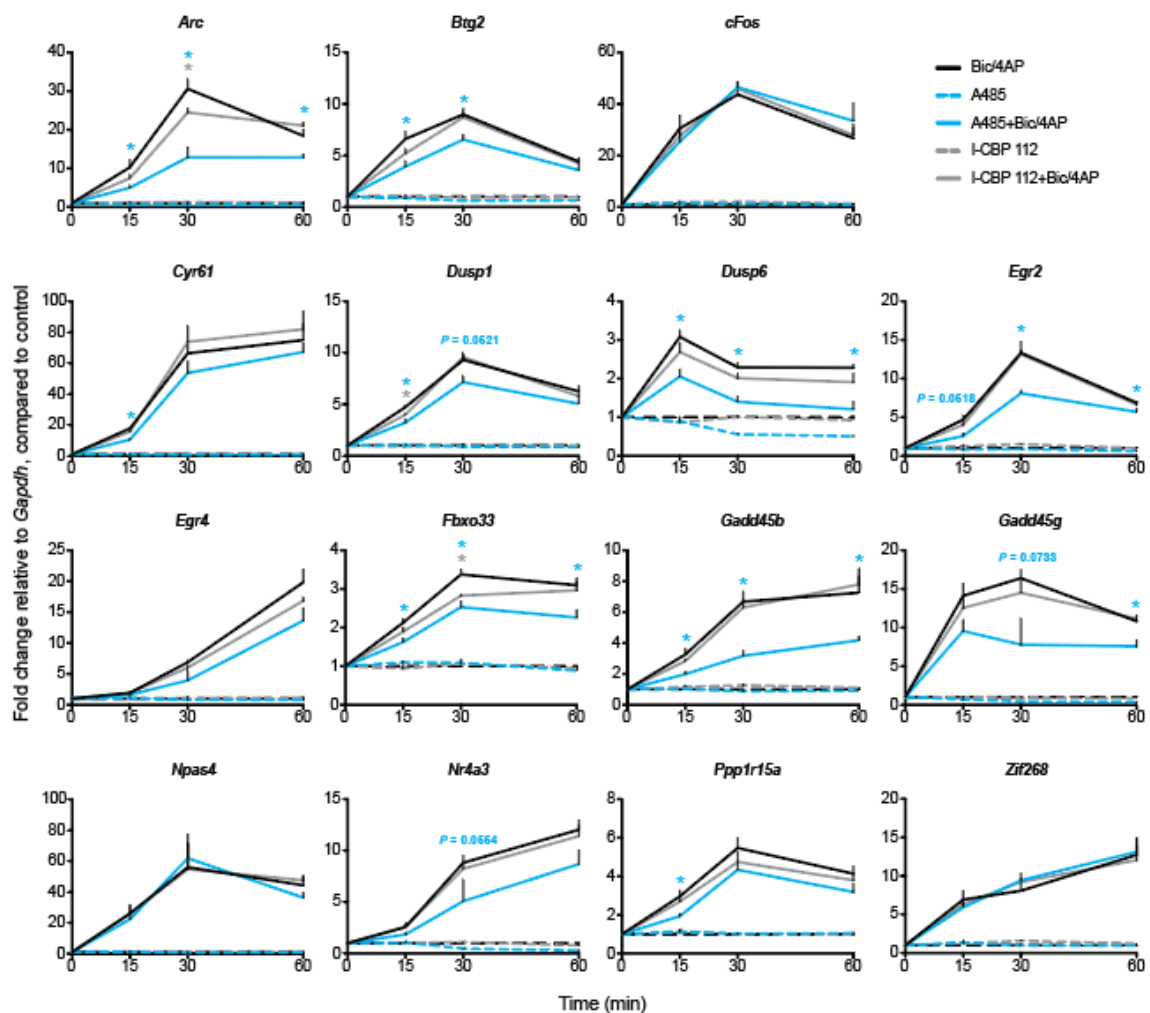


Figure 3-8 CBP HAT domain function is necessary for optimal expression of most rapid IEGs. A. Effect of CBP inhibitors on expression of rapid IEG pre-mRNA in neurons treated with Bic/4AP and collected at indicated time-points. Data represented as fold change compared to *Gapdh* as measured by qPCR; $N = 3$; * represents $p < 0.05$

genes. Further investigation will be necessary to understand if CaN signaling directly affects CBP HAT activity.

Our data suggests that CaN-mediated regulation of rapid IEG transcription may have unique temporal dynamics that differ from that of MAPK pathway-mediated regulation. We have shown that expression of some rapid IEGs can be induced by brief stimulation *in vitro*, and that it requires the MAPK pathway (Figure 3-9; adapted from Tyssowski, et al.,2018) which is supported by another report demonstrating the minimal signal strength required to induce transcription of *Arc* [Yu et al, 2017] in hippocampal neurons. Note that the expression of *Npas4* induced by brief activity is not completely abolished by MAPK inhibition, which is in line with our other *Npas4* findings (Figures 3-2 and 3-5). Based on our observation that inhibition of CaN activation does not affect early expression of some rapid IEGs (Figure 3-2), CaN signaling may or may not be involved in mediating expression of IEGs induced by brief activity. Further investigation will be necessary to adequately understand the temporal dynamics of CaN regulation in activity-induced transcription of rapid IEGs and these studies should be expanded to include delayed IEGs as well.

The results of our initial investigation into whether CaN signaling plays a role in regulating rapid IEG transcription suggested that most of these genes do rely on this pathway to some extent (Figure 3-2). However, the results of our inquiry into CRTTC1 as the potential downstream target of CaN functioning to regulate rapid IEG expression did not yield as broad of a phenotype across this cohort of genes as was expected (Figure 3-6). These results could suggest that CaN only functions through CRTTC1 to regulate expression of a fraction of these genes. This makes sense given that CaN has many other downstream targets known to regulate transcription, such as NFATs and MEFs, but more experiments would be necessary to draw concrete conclusions.

It has been shown that after nuclear import of dephosphorylated CRTTC1, the nuclear kinase SIK1 is responsible for phosphorylating nuclear CRTTC1 causing its export back to the cytoplasm [Li et al, 2009]. We hypothesized that if CaN is only functioning through CRTTC1 to regulate a few rapid IEGs (Figure 3-6), then those genes should present a distinct phenotype in response to SIK1 depletion. Our preliminary results suggest loss of SIK1 may cause increased expression of most rapid IEGs (Figure 3-9). Further experiments will be necessary to verify the results of this assay, as well as the efficiency of SIK1 knockdown. If this data holds true, it will be imperative to revisit the CRTTC1 depletion protocol and inquire whether SIK1 and CaN share other protein targets. It would also be interesting to expand this study to include delayed IEGs.

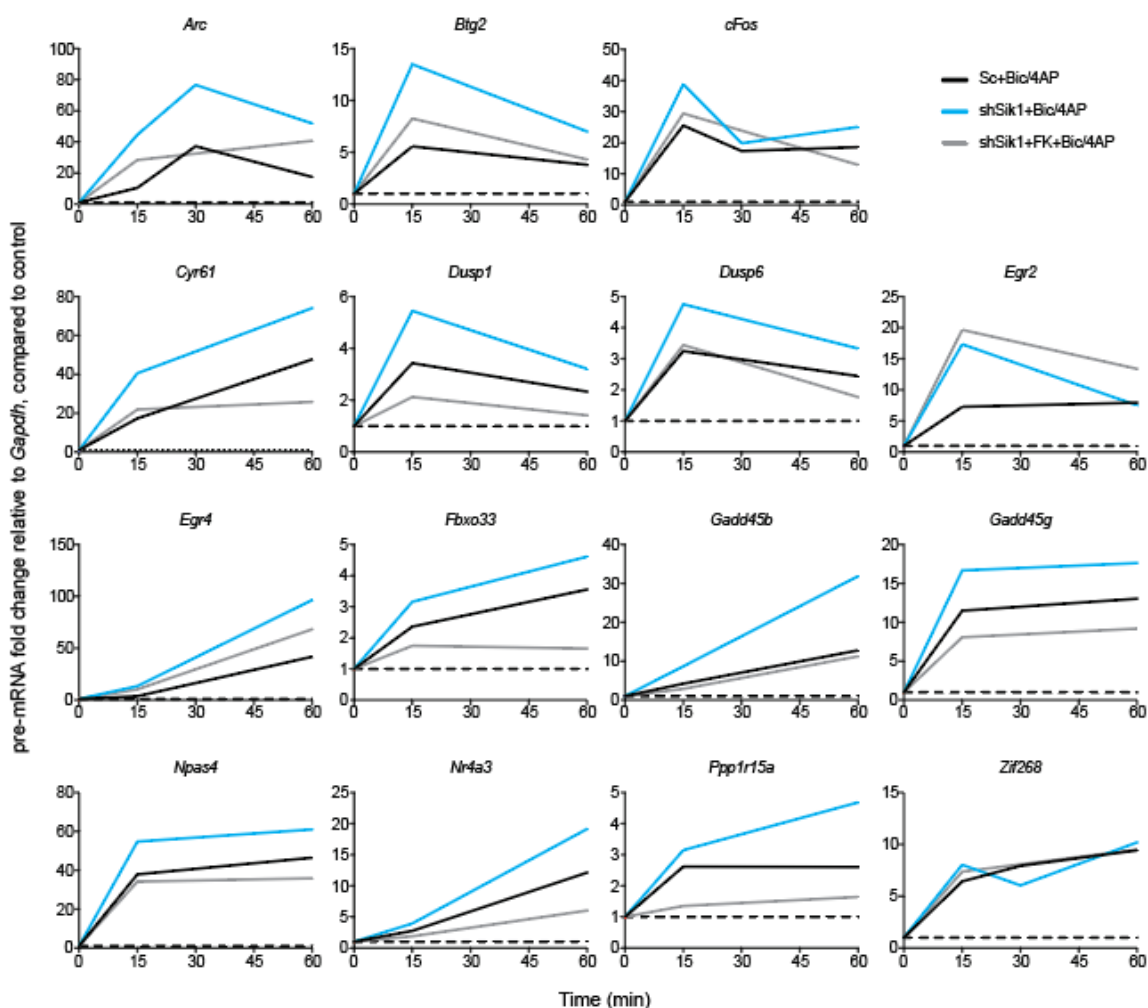


Figure 3-9 Preliminary investigation into the effect of Sik1 depletion on rapid IEG expression. Preliminary representation of rapid IEG pre-mRNA expression in neurons expressing an shRNA specific to Sik1. Cells were treated with Bic+4AP after 5-7 days of infection and collected at different time-points in the presence or absence of FK-506; data represented as fold change relative to *Gapdh*; $N = 1$

3.5 Materials and Methods

3.5.1 Isolation and culture of primary rat neurons

All experiments were carried out according to UCM and IACUC regulations. Cortical neurons were isolated from E18 Sprague Dawley rats, and single cell suspensions were prepared by triturating minced cortices through a fire-polished Pasteur pipet using Accutase (Invitrogen). Dissociated neurons were plated in Neurobasal medium (Invitrogen) supplemented with 0.5mM GlutaMAX-I (Invitrogen), 25 μ M glutamate (Sigma-Aldrich), and B27 (Invitrogen). Cells were maintained up to 14 days in a similar medium without glutamate. Cells were used for gene induction experiments between 10-14 days *in vitro* (DIV), at which time synapses have formed and are functional.

3.5.2 *Lentiviral prep and subsequent knockdown of target genes*

Bacteria expressing shRNA designed against desired targets (Sigma-Aldrich) were streaked on LB plates containing appropriate antibiotic and incubated at 37°C overnight. Single colonies were used to inoculate antibiotic-containing LB media, which was incubated at 37°C with shaking for 12-16 hours. Plasmid DNA was isolated using the GeneJET Plasmid Maxiprep kit (Thermo Scientific). To generate lentiviruses, HEK293T cells were plated in Dulbecco's Modified Eagle Medium (DMEM; Invitrogen) supplemented with 10% fetal bovine serum (FBS; Invitrogen) and split twice before being infected. To infect HEK293T cells, the culture media was first replaced with Opti-MEM (Invitrogen) + 10% FBS, and three separate plasmids (shRNA-containing plasmid, VSV-G envelope plasmid, Gag-Pol packaging plasmid) were diluted in the new media. Cells were maintained at 37°C with 5% CO₂, and supernatant containing shRNA was collected 40-48 hours after multi-plasmid infection. To knockdown target genes, supernatant containing appropriate shRNA was diluted in primary neuron culture media at DIV 5-8, and experiments were routinely done 4-7 days after infection.

3.5.3 *In vitro gene induction assays*

Assays involving Bic+4AP to excite synaptically, as well as TTX+PMA to drive transcription intracellularly (both described in Chapter 2) were used in this study. Brief activity experiments involved exposing cortical neuron cultures to Bic+4AP for a short time (10-30 seconds) followed by a washout with media containing TTX to stop synaptic transmission. Cells were collected at various time-points after initial stimulation.

3.5.4 *Western blotting and imaging*

Protein samples were isolated in RIPA buffer, denatured in Laemeli Buffer (BioRad) + β -mercaptoethanol on a heat block at 95°C for 5 min, and resolved on 4-20%, 4-15%, or 8-16% Mini-PROTEAN gels (BioRad) in 1X Tris/Glycine/SDS (BioRad) buffer. The BioRad TBT RTA kit and protocol were used to transfer resolved proteins onto LV PVDF membranes (BioRad). Membranes were incubated at 4°C overnight with primary antibodies in 1X TBS-T (Invitrogen) with 0.5% bovine serum albumin (BSA; Fisher Scientific), washed thrice with 1X TBS-T, incubated on a rocker with appropriate secondary antibody at room temperature for 30-60 minutes, washed thrice with 1X TBS-T, and imaged using the BioRad ChemiDoc Imaging System.

3.5.5 *Statistical analysis*

Biological replicates for each figure are indicated as *N* in corresponding figure legends. Error bars represent standard error of mean throughout this article. Statistical comparison of datasets was performed with the two-tailed Student's *t*

test (with Bonferroni corrections for multiple comparisons) unless otherwise stated in the figure legend.

Chapter 4: CONCLUSION

Neurodevelopmental and cognitive studies have reported that dysregulated IEG expression contributes to increasingly common brain disorders, including Autism and Schizophrenia. To better understand mechanisms regulating IEG expression in neurons, we investigated multiple factors whose contribution to IEG expression had yet to be investigated or was not completely understood. The first of these factors was the histone variant H2A.Z, which is comprised of two structurally similar hypervariants, H2A.Z.1 and H2A.Z.2. Although these hypervariants were described in 2009 [Dryhurst et al, 2009], they have widely been considered functionally redundant, likely due to the lack of tools available to distinguish between them. Using hypervariant-specific shRNA developed in our lab [Dunn et al, 2017], we demonstrated multiple non-redundant effects of H2A.Z.1 and H2A.Z.2 in transcriptional regulation of IEGs: (1) H2A.Z.1 and H2A.Z.2 depletion differently influence activity-induced *Arc* transcription kinetics; (2) in resting neurons, H2A.Z.2, but not H2A.Z.1, is required near the *Arc* TSS for RNA Pol II pausing; (3) activity-induced transcription of certain IEGs is sensitive to depletion of only one of the two hypervariants (e.g., *Btg2* and *Dusp1* response is less after H2A.Z.2, but not H2A.Z.1, knockdown); and (4) certain IEGs appear to be differentially sensitive to one or both hypervariants in a context-dependent manner (*Fbxo33* and *Maff* after H2A.Z.1 depletion, *Fam46a* after loss of H2A.Z.2). Further investigation of the role(s) of these hypervariants in neurodevelopment suggest that H2A.Z.1 and H2A.Z.2 may differentially regulate neural progenitor cell cycle dynamics and neuronal differentiation. Taken together, the data presented strongly suggest that H2A.Z hypervariants have important, nonredundant roles and/or functional specificity that should be considered for a full understanding of the role of H2A.Z in IEG transcription and neurodevelopment.

Messages encoded in patterns of membrane depolarization are conveyed to the nucleus via series' of protein interactions acting in a cascade. These calcium-induced signaling pathways facilitate the orchestration of nuclear events by neuronal activity. It has been reported that the MAPK pathway is required for rapid IEG transcription, but that some IEGs are still expressed at low levels in the presence of a MAPK inhibitor [Tyssowski et al, 2018] suggesting that there may be more signaling pathways involved in regulating rapid IEG transcription. We investigated the contribution of CaN signaling to rapid IEG expression and report here that CaN signaling is necessary for optimal expression of most rapid IEGs. Our data suggest that CaN may regulate individual rapid IEGs via interaction with different downstream targets, however future experiments will be necessary to delineate which CaN targets function to regulate expression of each gene. Further investigation into regulation of IEG expression revealed that, like CaN signaling, CBP HAT activity is necessary for optimal expression of most rapid

IEGs and *SARE* eRNA. Follow-up will be necessary to understand if CaN signaling interacts with CBP directly, or if these factors act in parallel to regulate gene expression.

The work presented in this dissertation contributes to our overall understanding of how individual IEGs are regulated by H2A.Z hypervariants, as well as different calcium-dependent signaling cascades (see Figure 4-1). These results highlight the fact that there is likely no all-encompassing transcriptional mechanism regulating IEG transcription. While this study focused on contributions of H2A.Z hypervariants and CaN signaling on the regulation of IEG expression, it is likely that each gene is uniquely regulated by a combination of signaling cascades that act on many more epigenetic factors associated with promoters and enhancers. It is also likely that each gene possesses a unique combination of genetic elements that define its epigenetic landscape. A complete understanding of the molecular dynamics governing transcriptional regulation will require that future studies investigate the interaction of regulatory elements at different cellular levels, or compartments (i.e. membrane, cytoplasm, nucleus).

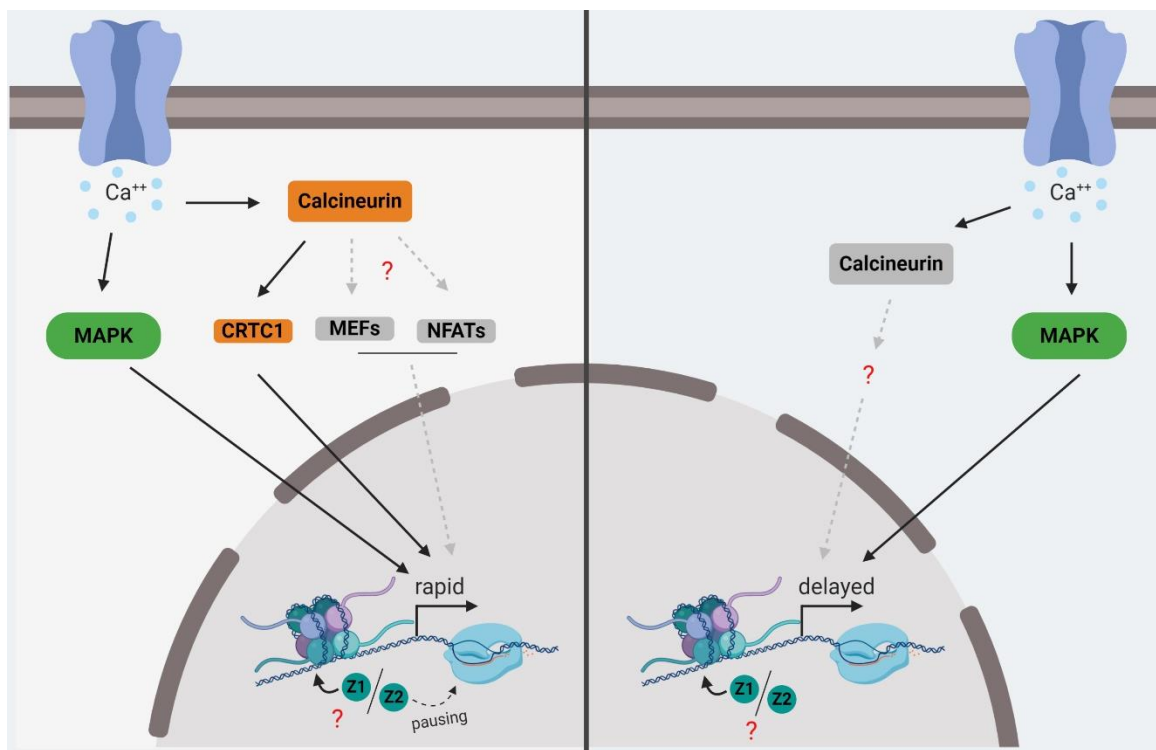


Figure 4-1. Summary of Findings

As we continue to define how expression of individual genes is regulated, it will be important to consider how opposing molecular processes work to maintain a balance of resources in the brain. Neuronal plasticity is a great example of how the coordinated action of kinases and phosphatases maintain equilibrium of a

system [Woolfrey et al, 2015]. This pattern seems to hold true when we zoom in to more specific molecular processes like transcriptional regulation. For example, the MAPK pathway recruits Pol II, contributing to activation of transcription, and our data demonstrates that the repressive mechanism blocked by inhibition of protein translation (resulting in superinduction) does not act via the MAPK pathway, but in fact may act via CaN phosphatase signaling. However, it will be important going forward to consider that kinases and phosphatases could each contribute to both the positive and negative regulation of a system, depending on the function of the particular downstream targets they activate. For example, preliminary data presented here demonstrates that SIK1 may contribute to repression of some rapid IEGs, likely via phosphorylation and subsequent export of CRTC1 from the nucleus. It has been shown, however, that CRTC1 (a downstream target of CaN) promotes transcription of *Sik1* [Jagannath et al, 2013]. This example demonstrates the potential for CaN activation to be contributing to both activation and repression of rapid IEG expression. A full appreciation for the nuances governing transcriptional dynamics will be necessary if future tool building efforts aim to target transcriptional processes.

The data presented in this dissertation highlight the necessity for continued efforts focused on teasing out the mechanisms regulating transcription of different IEGs in hopes of one day developing tools to combat neurodevelopmental and cognitive disorders.

REFERENCES

- Adelman, K and Lis, J T. "Promoter-proximal pausing of RNA polymerase II: emerging roles in metazoans." *Nat Rev.* vol. 13. (2012), doi:10.1038/nrg3293
- Alatwi, H E and Downs, J A. "Removal of H2A.Z by INO80 promotes homologous recombination." *EMBO Rep* vol. 16. (2015), doi: 10.15252/embr.201540330
- Altar, C A et al. "Electroconvulsive seizures regulate gene expression of distinct neurotrophic signaling pathways." *J. Neurosci.* vol. 24. (2004), doi:10.1523/JNEUROSCI.5377-03.2004
- Andersson, R et al. "A unified architecture of transcriptional regulatory elements." *Trends Genet.* vol. 31. (2015), doi:10.1016/j.tig.2015.05.007
- Bachmann, C et al. "mSWI/SNF (BAF) Complexes Are Indispensable for the Neurogenesis and Development of Embryonic Olfactory Epithelium." *PLoS genetics* vol. 12. (2016), doi:10.1371/journal.pgen.1006274
- Bading, H. "Regulation of gene expression in hippocampal neurons by distinct calcium signaling pathways." *Science.* vol. 260. (1993), doi:10.1126/science.8097060
- Bannister, A J and Kouzarides T. "The CBP co-activator is a histone acetyltransferase." *Nature* vol. 384. (1996), doi:10.1038/384641a0
- Berridge, M J. "Neuronal calcium signaling." *Neuron.* vol. 21. (1998), doi: 10.1016/s0896-6273(00)80510-3
- Biterge, B. & Schneider, R. Histone variants: key players of chromatin. *Cell Tissue Res* (2014) 356: 457. <https://doi.org/10.1007/s00441-014-1862-4>
- Bittinger, M A et al. "Activation of cAMP response element-mediated gene expression by regulated nuclear transport of TORC proteins." *Curr. Biol.* vol. 14. (2004), doi:10.1016/j.cub.2004.11.002
- Bruce, K et al. "The replacement histone H2A.Z in a hyperacetylated form is a feature of active genes in the chicken." *Nucleic Acids Res* vol. 33. (2005), doi:10.1093/nar/gki874
- Carelli, F N et al. "Repurposing of promoters and enhancers during mammalian evolution." *Nat. Commun.* vol. 9. (2018), doi:10.1038/s41467-018-06544-z
- Carullo, N V N and Day, J J. "Genomic Enhancers in Brain Health and Disease." *Genes* vol. 10. (2019), doi:10.3390/genes10010043

Chen, Y et al. "NS21: re-defined and modified supplement B27 for neuronal cultures". *J Neurosci Methods*. vol. 171. (2008), doi:10.1016/j.jneumeth.2008.03.013

Chin, E R et al. "A calcineurin-dependent transcriptional pathway controls skeletal muscle fiber type." *Genes & development* vol. 12,16 (1998), doi:10.1101/gad.12.16.2499

Cochran, B H et al. "Molecular cloning of gene sequences regulated by platelet-derived growth factor." *Cell* vol. 33. (1983), doi:10.1016/0092-8674(83)90037-5

Conkright, M D et al. "TORCs: transducers of regulated CREB activity." *Molecular Cell* vol. 12. (2003), doi:10.1016/j.molcel.2003.08.013

Day, D S et al. "Comprehensive analysis of promoter-proximal RNA polymerase II pausing across mammalian cell types." *Genome Biol* vol. 17. (2016), doi:10.1186/s13059-016-0984-2

Doyen, Cécile-Marie et al. "Dissection of the unusual structural and functional properties of the variant H2A.Bbd nucleosome." *The EMBO journal* vol. 25,18 (2006): 4234-44. doi:10.1038/sj.emboj.7601310

Dryhurst, D et al. "Characterization of the histone H2A.Z-1 and H2A.Z-2 isoforms in vertebrates." *BMC Biol* vol. 7. (2009), doi:10.1186/1741-7007-7-86

Dunn, C J et al. "Histone Hypervariants H2A.Z.1 and H2A.Z.2 Play Independent and Context-Specific Roles in Neuronal Activity-Induced Transcription of *Arc/Arg3.1* and Other Immediate Early Genes." *eNeuro* vol. 4. (2017), doi:10.1523/ENEURO.0040-17.2017

Faast, R et al. "Histone variant H2A.Z is required for early mammalian development." *Curr Biol* vol. 11. (2001)

Farris, S D et al. "Transcription-induced chromatin remodeling at the c-myc gene involves the local exchange of histone H2A.Z." *J Biol Chem* vol. 280 (2005), doi:10.1074/jbc.M501784200

Filipescu, D et al. "Developmental roles of histone H3 variants and their chaperones." *Trends Genet* vol. 29. (2013), doi:10.1016/j.tig.2013.06.002

Flavell, S W et al. "Activity-dependent regulation of MEF2 transcription factor suppresses excitatory synapse number." *Science* vol. 311. (2005), doi:10.1126/science.1122511

- Gallo, Francisco T et al. "Immediate Early Genes, Memory and Psychiatric Disorders: Focus on c-Fos, Egr1 and Arc." *Frontiers in behavioral neuroscience* vol. 12 79. (2018), doi:10.3389/fnbeh.2018.00079
- Ghosh, A et al. "Requirement for BDNF in activity-dependent survival of cortical neurons." *Science*. vol. 263. (1994), doi: 10.1126/science.7907431
- Ginty, D D. "Calcium regulation of gene expression: isn't that spatial?." *Neuron*. vol. 18. (1997), doi: 10.1016/s0896-6273(00)80258-5
- Graef, I et al. "L-type calcium channels and GSK-3 regulate the activity of NF-ATc4 in hippocampal neurons." *Nature* vol 401. (1999), doi:10.1038/44378
- Greenberg, M E et al. "Stimulation of neuronal acetylcholine receptors induces rapid gene transcription." *Science*. vol. 234. (1986), doi:10.1126/science.3749894
- Greer and Greenberg. "From synapse to nucleus: Calcium-dependent gene transcription in the control of synapse development and function." *Neuron* vol. 59. (2008), doi:10.1016/j.neuron.2008.09.002
- Gursoy-Yuzugullu, O et al. "Histone chaperone Anp32e removes H2A.Z from DNA double-strand breaks and promotes nucleosome reorganization and DNA repair." *Proc Natl Acad Sci USA* vol. 112. (2015), doi:10.1073/pnas.1504868112
- Guzowski, J F et al. "Environment-specific expression of the immediate-early gene Arc in hippocampal neuronal ensembles." *Nat Neurosci* vol. 2. (1999)
- Hong, S J et al. "Identification and analysis of plasticity-induced late-response genes." *Proc. Natl. Acad. Sci. USA*. vol. 101 (2004), doi:10.1073/pnas.0305170101
- Horikoshi, N et al. "Structural polymorphism in the L1 loop regions of human H2A.Z.1 and H2A.Z.2." *Acta Crystallogr D Biol Crystallogr* vol. 69. (2013), doi:10.1107/S090744491302252X
- Hunt, S et al. "Induction of c-fos-like protein in spinal cord neurons following sensory stimulation." *Nature*. vol. 328. (1987), doi:10.1038/328632a0
- Husi, H et al. "Proteomic analysis of NMDA receptor-adhesion protein signaling complexes." *Nat. Neurosci*. Vol. 3. (2000), doi:10.1038/76615
- Jagannath, A et al. "The CRTCL1-SIK1 pathway regulates entrainment of the circadian clock." *Cell* vol. 154. (2013), doi:10.1016/j.cell.2013.08.004

Jonas, P and Burnashev, N. "Molecular mechanisms controlling calcium entry through AMPA-type glutamate receptor channels." *Neuron*. vol. 15. (1995), doi:10.1016/0896-6273(95)90087-x

Kim, T et al. "Widespread transcription at neuronal activity-regulated enhancers." *Nature* vol. 465,7295 (2010): 182-7. doi:10.1038/nature09033

Kwak, H and Lis, J T. "Control of transcriptional elongation." *Annu Rev Genet* vol. 47. (2013), doi:10.1146/annurev-genet-110711-155440

Kwok, R P et al. "Nuclear protein CBP is a coactivator for the transcription factor CREB." *Nature* vol. 370. (1994), doi:10.1038/370223a0

Lau, L F and Nathans, D. "Expression of a set of growth-related immediate early genes in BALB/c 3T3 cells: coordinate regulation with c-fos or c-myc." *Proc Natl Acad Sci U S A* vol. 84. (1987), doi:10.1073/pnas.84.5.1182

Lee, K et al. "Dynamic enhancer-gene body contacts during transcription elongation." *Genes Dev* vol. 29. (2015)

Lessard, J et al. "An essential switch in subunit composition of a chromatin remodeling complex during neural development." *Neuron* vol. 55. (2007), doi:10.1016/j.neuron.2007.06.019

Li, G et al. "Extensive Promoter-Centered Chromatin Interactions Provide a Topological Basis for Transcription Regulation." *Cell*. vol. 148. (2012), doi:10.1016/j.cell.2011.12.014

Li, H et al. "Identification of calcium- and nitric oxide-regulated genes by differential analysis of library expression (DAzLE)." *Proc. Natl. Acad. Sci. USA*. vol. 101 (2004), doi:10.1073/pnas.0305145101

Li, S et al. "TORC1 regulates activity-dependent CREB-target gene transcription and dendritic growth of developing cortical neurons." *Journal of Neuroscience*. vol. 29. (2009), doi:10.1523/jneurosci.2296.-08.2009

Malik, A N et al. "Genome-wide identification and characterization of functional neuronal activity-dependent enhancers." *Nature neuroscience* vol. 17,10 (2014): 1330-9. doi:10.1038/nn.3808

Mao, Z et al. "Anp32e, a higher eukaryotic histone chaperone directs preferential recognition for H2A.Z." *Cell Res*. vol. 24. (2014), doi:10.1038/cr.2014.30

Mao and Wiedmann. "Calcineurin enhances MEF2 DNA binding activity in calcium-dependent survival of cerebellar granule neurons." *J. Biol. Chem*. vol 274. (1999), doi:10.1074/jbc.274.43.31102

Marballi, K K. "Immediate Early Genes Anchor a Biological Pathway of Proteins Required for Memory Formation, Long-Term Depression and Risk for Schizophrenia." *Frontiers in behavioral neuroscience* vol. 12. (2018), doi:10.3389/fnbeh.2018.00023

Matsuda, R et al. "Identification and characterization of the two isoforms of the vertebrate H2A.Z histone variant." *Nucleic Acids Res* vol. 38. (2010), doi:10.1093/nar/gkq171

Maze, I et al. "Every amino acid matters: essential contributions of histone variants to mammalian development and disease." *Nat Rev* vol. 15. (2014), doi:10.1038/nrg3673

Maze, I et al. "Critical role of histone turnover in neuronal transcription and plasticity." *Neuron* vol. 87. (2015), doi:10.1016/j.neuron.2015.06.014

Michod, D et al. "Calcium-dependent dephosphorylation of the histone chaperone DAXX regulates H3.3 loading and transcription upon neuronal activation." *Neuron* vol. 74. (2012), doi:10.1016/j.neuron.2012.02.021

Morgan, J I et al. "Mapping patterns of c-fos expression in the central nervous system after seizure." *Science*. vol. 237. (1987), doi:10.1126/science.3037702

Nedivi, E et al. "Numerous candidate plasticity-related genes revealed by differential cDNA cloning." *Nature*. vol. 363. (1993), doi:10.1038/363718a0

Nguyen, T A et al. "High-throughput functional comparison of promoter and enhancer activities." *Genome Res*. vol. 26. (2016), doi:10.1101/gr.204834.116

Obri, A et al. "ANP32E is a histone chaperone that removes H2A.Z from chromatin." *Nature* vol. 505. (2014), doi:10.1038/nature12922

Owen-Hughes, T and Gkikopoulos, T. "Making sense of transcribing chromatin." *Curr Opin Cell Biol*. vol. 24. (2012), doi:10.1016/j.ceb.2012.02.003

Papadia, S et al. "Nuclear Ca²⁺ and the cAMP response element-binding protein family mediate a late phase of activity-dependent neuroprotection." *J Neurosci* vol. 25. (2005), doi:10.1523/JNEUROSCI.5019-04.2005

Park, C S et al. "Molecular network and chromosomal clustering of genes involved in synaptic plasticity in the hippocampus." *J. Biol. Chem*. vol. 281. (2006), doi:10.1074/jbc.M605876200

- Raisner, R et al. "Enhancer Activity Requires CBP/P300 Bromodomain-Dependent Histone H3K27 Acetylation." *Cell Reports* vol. 24. (2018), doi:10.1016/j.celrep.2018.07.041
- Raisner, R M and Madhani, H D. "Patterning chromatin: form and function for H2A.Z variant nucleosomes." *Curr Opin Genet Dev* vol. 16. (2006), doi:10.1016/j.gde.2006.02.005
- Rao, V R et al. "AMPA receptors regulate transcription of the plasticity-related immediate-early gene *Arc*." *Nat Neurosci* vol. 9. (2006)
- Rosen, L B et al. "Membrane depolarization and calcium influx stimulate MEK and MAP kinase via activation of Ras." *Neuron* vol. 12. (1994)
- Rusak, B et al. "Light pulses that shift rhythms induce gene expression in the suprachiasmatic nucleus." *Science*. vol. 248. (1990), doi:10.1126/science.2112267
- Saha, R N et al. "Rapid activity-induced transcription of *Arc* and other IEGs relies on poised RNA polymerase II." *Nat Neurosci*. vol. 14. (2011), doi:10.1038/nn.2839
- Schultz, H et al. "PMA-induced activation of the p42/44ERK- and p38RK-MAP kinase cascades in HL-60 cells is PKC dependent but not essential for differentiation to the macrophage-like phenotype." *J Cell Physiol* vol. 173. (1997), doi:10.1002/(SICI)1097-4652(199712)173:3<AID-JCP2>3.0.CO;2-Q
- Shen, T et al. "Brain-specific deletion of histone variant H2A.z results in cortical neurogenesis defects and neurodevelopmental disorder." *Nucleic acids research* vol. 46. (2018), doi:10.1093/nar/gkx1295
- Soboleva, T A et al. "Histone variants at the transcription start-site." *Trends Genet*. vol. 30. (2014), doi:10.1016/j.tig.2014.03.002
- Talbert, P B et al. "A unified phylogeny-based nomenclature for histone variants." *Epigenetics Chromatin* vol. 5. (2012), doi:10.1186/1756-8935-5-7
- Talbert, P., Henikoff, S. Histone variants on the move: substrates for chromatin dynamics. *Nat Rev Mol Cell Biol* 18, 115–126 (2017) doi:10.1038/nrm.2016.148
- Teves, S S et al. "Transcribing through the nucleosome." *Trends Biochem Sci*. vol. 39. (2014), doi:10.1016/j.tibs.2014.10.004
- Titov, D V et al. "XPB, a subunit of TFIIH, is a target of the natural product triptolide." *Nat Chem Biol* vol. 7. (2011)

- Tolias, K F et al. "The Rac1-GEF Tiam1 couples the NMDA receptor to the activity-dependent development of dendritic arbors and spines." *Neuron* vol. 45. (2005), doi:10.1016/j.neuron.2005.01.024
- Tolstorukov, Michael Y et al. "Histone variant H2A.Bbd is associated with active transcription and mRNA processing in human cells." *Molecular cell* vol. 47,4 (2012): 596-607. doi:10.1016/j.molcel.2012.06.011
- Tyssowski, K M et al. "Different Neuronal Activity Patterns Induce Different Gene Expression Programs." *Neuron* vol. 98. (2018), doi:10.1016/j.neuron.2018.04.001
- Valdés-Mora, F et al. "Acetylation of H2A.Z is a key epigenetic modification associated with gene deregulation and epigenetic remodeling in cancer." *Genome Res.* vol. 22. (2012), doi:10.1101/gr.118919.110
- Vardabasso, C et al. "Histone variant H2A.Z.2 mediates proliferation and drug sensitivity of malignant melanoma." *Mol Cell* vol. 59. (2015), doi:10.1016/j.molcel.2015.05.009
- Weber, C M and Henikoff, S. "Histone variants: dynamic punctuation in transcription." *Genes Dev.* vol. 28. (2014), doi:10.1101/gad.238873.114
- Webster, N et al. "The yeast UASG is a transcriptional enhancer in human hela cells in the presence of the GAL4 trans-activator." *Cell.* vol. 52. (1988), doi:10.1016/0092-8674(88)90505-3
- Westenbroek, R E et al. "Biochemical properties and subcellular distribution of an N-type calcium channel alpha 1 subunit." *Neuron.* vol. 9 (1992), doi:10.1126/science.7907431
- Wiegert, J S and Bading, H. "Activity-dependent calcium signaling and ERK-MAP kinases in neurons: a link to structural plasticity of the nucleus and gene transcription regulation." *Cell Calcium* vol. 49. (2011), doi:10.1016/j.ceca.2010.11.009
- Woolfrey, K M and Dell'Acqua, M L. "Coordination of Protein Phosphorylation and Dephosphorylation in Synaptic Plasticity." *The Journal of biological chemistry* vol. 290,48 (2015), doi:10.1074/jbc.R115.657262
- Wrattling, D et al. "A conserved function for the H2A.Z C terminus." *J Biol Chem.* vol. 287. (2012), doi:10.1074/jbc.M111.317990
- Wu, J I et al. "Regulation of dendritic development by neuron-specific chromatin remodeling complexes." *Neuron* vol. 56. (2007), doi:10.1016/j.neuron.2007.08.021

- Wu, X and Brewer, G. "The regulation of mRNA stability in mammalian cells: 2.0." *Gene* vol. 500. (2012), doi:10.1016/j.gene.2012.03.021
- Xu, W et al. "Individual CREB-target genes dictate usage of distinct cAMP-responsive coactivation mechanisms." *The EMBO journal* vol. 26,12 (2007), doi:10.1038/sj.emboj.7601734
- Yang, Y et al. "Chromatin remodeling inactivates activity genes and regulates neural coding." *Science* vol. 353. (2016), doi:10.1126/science.aad4225
- Yu, Yan et al. "One nuclear calcium transient induced by a single burst of action potentials represents the minimum signal strength in activity-dependent transcription in hippocampal neurons." *Cell Calcium* vol. 65. (2017), doi:10.1016/j.ceca.2017.03.003
- Zabidi, M A et al. "Enhancer-core-promoter specificity separates developmental and housekeeping gene regulation." *Nature*. vol. 518. (2015), doi:10.1038/nature13994
- Zhang, T et al. "CaMKII δ isoforms differentially affect calcium handling but similarly regulate HDAC/MEF2 transcriptional responses." *J. Biol. Chem.* vol. 282. (2007), doi:10.1074/jbc.M707083200
- Zhen Sun, Emily Bernstein; Histone variant macroH2A: from chromatin deposition to molecular function. *Essays Biochem* 23 April 2019; 63 (1): 59–74. doi: <https://doi.org/10.1042/EBC20180062>
- Zlatanova, J and Thakar, A. "H2A.Z: view from the top." *Structure* vol. 16. (2008), doi:10.1016/j.str.2007.12.008
- Zovkic, I B et al "Histone H2A.Z subunit exchange controls consolidation of recent and remote memory." *Nature* vol. 515. (2014), doi:10.1038/nature137.

